BIOCHEMISTRY
including biophysical chemistry & molecular biology

New Concept

pubs.acs.org/biochemistry

Cellular Assays for Ferredoxins: A Strategy for Understanding Electron Flow through Protein Carriers That Link Metabolic Pathways

Joshua T. Atkinson,[†] Ian Campbell,[‡] George N. Bennett,[§,∥] and Jonathan J. Silberg*[,§,⊥]

[†]Systems, Synthetic, and Physical Biology Graduate Program, Rice University, MS-180, 6100 Main Street, Houston, Texas 77005, United States

[‡]Biochemistry and Cell Biology Graduate Program, Rice University, MS-140, 6100 Main Street, Houston, Texas 77005, United States

[§]Department of Biosciences, Rice University, MS-140, 6100 Main Street, Houston, Texas 77005, United States

[∥]Department of Chemical and Biomolecular Engineering, Rice University, MS-362, 6100 Main Street, Houston, Texas 77005, United States

[⊥]Department of Bioengineering, Rice University, MS-142, 6100 Main Street, Houston, Texas 77005, United States

Supporting Information

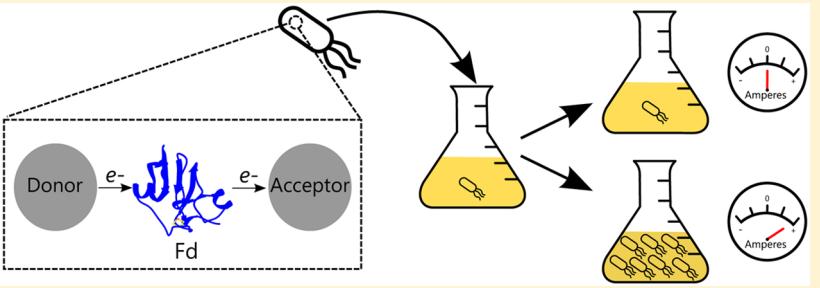

ABSTRACT: The ferredoxin (Fd) protein family is a structurally diverse group of iron−sulfur proteins that function as electron carriers, linking biochemical pathways important for energy transduction, nutrient assimilation, and primary metabolism. While considerable biochemical information about individual Fd protein electron carriers and their reactions has been acquired, we cannot yet anticipate the proportion of electrons shuttled between different Fd-partner proteins within cells using biochemical parameters that govern electron flow, such as holo-Fd concentration, midpoint potential (driving force), molecular interactions (affinity and kinetics), conformational changes (allostery), and off-pathway electron leakage (chemical oxidation). Herein, we describe functional and structural gaps in our Fd knowledge within the context of a sequence similarity network and phylogenetic tree, and we propose a strategy for improving our understanding of Fd sequence−function relationships. We suggest comparing the functions of divergent Fds within cells whose growth, or other measurable output, requires electron transfer between defined electron donor and acceptor proteins. By comparing Fd-mediated electron transfer with biochemical parameters that govern electron flow, we posit that models that anticipate energy flow across Fd interactomes can be built. This approach is expected to transform our ability to anticipate Fd control over electron flow in cellular settings, an obstacle to the construction of synthetic electron transfer pathways and rational optimization of existing energy-conserving pathways.

■ ELECTRON FLOW AND METABOLISM

Metabolism arises from a complex network of biochemical transformations that control the flux of carbon and energy from nutrients into biomass. These networks are subject to stratified layers of regulation that organisms use to dynamically maximize the trade-off between metabolic flexibility and efficiency to suit their environmental needs. Cells use two major strategies to regulate carbon and electron fluxes. Cells switch on and off the production of enzymes and redox proteins, and they use post-translational reactions to tune the reaction fluxes controlled by these biomolecules.[1,2] The processes that control enzyme and redox protein levels (transcription, translation, and degradation) all function on relatively long time scales (minutes to hours). This strategy of controlling protein levels is energy intensive, accounting for approximately two-thirds of cellular ATP consumption under exponential growth conditions.[3] Post-translational reactions, in contrast, allow for more rapid tuning of metabolic fluxes (microseconds to milliseconds) without requiring high ATP costs.

Our understanding of microbial metabolism is now sufficient to routinely direct carbon flow toward high-value chemicals through static and dynamic manipulations of metabolic pathways,[4] albeit with variable carbon and energy efficiencies. Carbon flux through central metabolism can be modulated by expressing non-native proteins that divert carbon to product synthesis once biomass has accumulated[5,6] or altering transcription

Received: August 11, 2016
Revised: November 18, 2016
Published: November 21, 2016

DOI: 10.1021/acs.biochem.6b00831
Biochemistry 2016, 55, 7047−7064

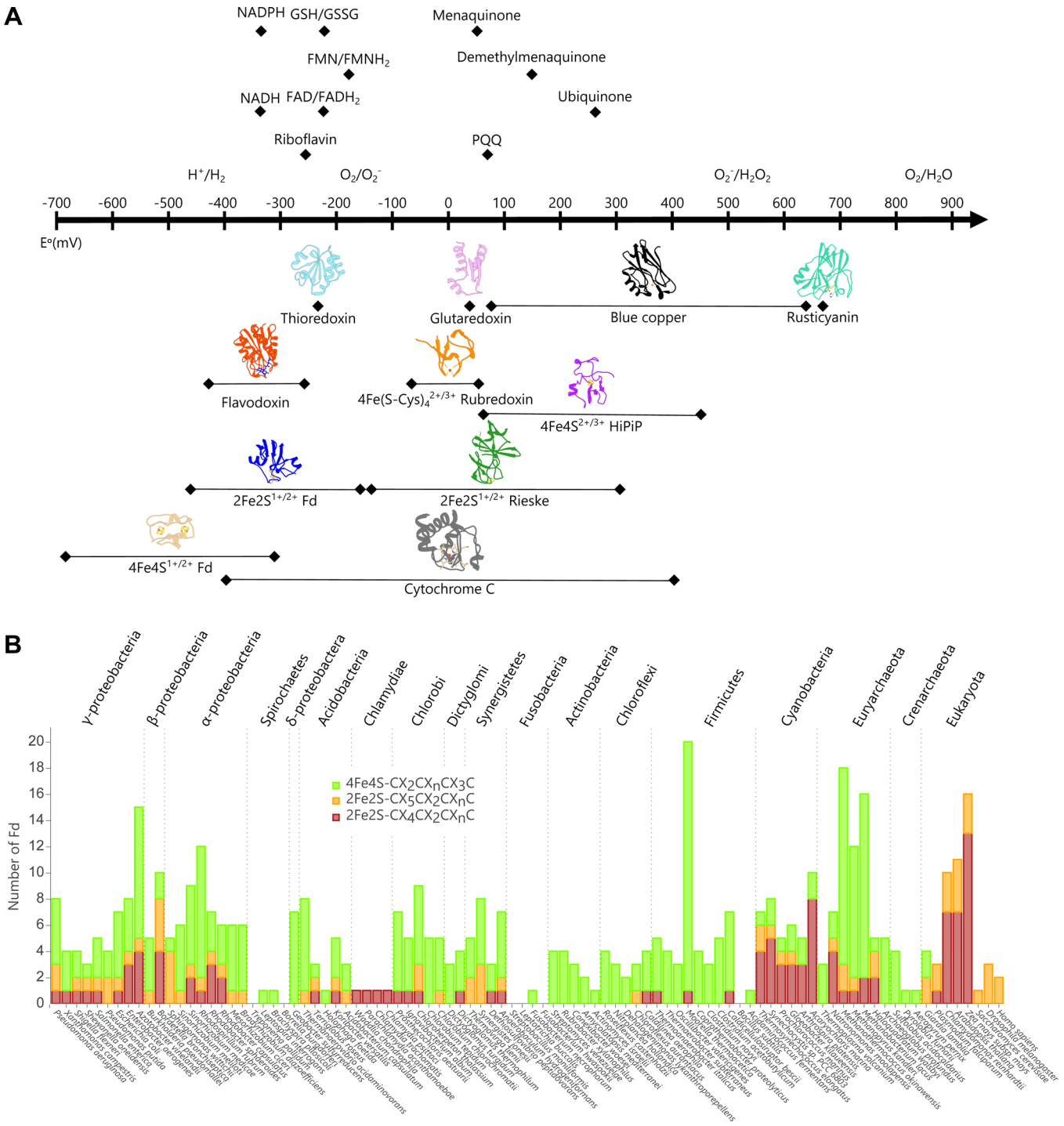

Figure 1. Biological electron carriers that function as redox hubs in cells. (A) Comparison of the reduction potential ranges for small-molecule and protein electron carriers. Diamonds indicate the range or values of observed midpoint reduction potentials. (B) Prevalence of small ferredoxins in 74 bacteria, 10 archaea, and 8 eukaryotes. Ferredoxins were mined from representative annotated proteomes in the NCBI genome database.[142] Proteins were selected on the basis of being annotated as "ferredoxin", "putidaredoxin", or "adrenodoxin", possessing documented ferredoxin iron–sulfur cluster binding moieties,[40,80] and consisting of ≤200 amino acids. A subscript n following X denotes the variable number of amino acids.

to: (i) respond to variations in pathway intermediates,[7] (ii) decrease noise in enzyme concentrations,[8] and (iii) couple growth rate to product synthesis.[9] Pathway efficiency can also be tuned post-translationally by increasing local enzyme concentrations with engineered macromolecular interactions[10−13] and limiting fluxes at specific enzymes by engineering allosteric responses and feedback control.[1,8,14,15] While pathway productivity improvements have been achieved in many studies, they typically have focused on alterations in carbon flux alone, rather than targeting both energy and carbon flux in tandem.

Genetic modifications that alter carbon metabolism can lead to the accumulation of reduced or oxidized cofactors that cause global imbalances. In an effort to rebalance electron flow to avoid pathway-flux limitations arising from cofactor perturbations, several studies have examined whether the redox state of electron-carrying cofactors can be tuned by modifying the levels

DOI: 10.1021/acs.biochem.6b00831
Biochemistry 2016, 55, 7047−7064

of enzymes that produce[16] and regenerate[17,18] those cofactors. However, these studies have not yet revealed simple and generalizable approaches for controlling electron flux. In part, this challenge exists because a small number of carriers often mediate electron transfer between large numbers of partner proteins. In *Escherichia coli*, the major electron carriers are the nicotinamide adenine dinucleotides, NADH and NADPH, with these carriers being involved in >100 metabolic reactions.[19] In addition, the terminal electron carrier for aerobic respiration (quinone Q8) is involved in two dozen reactions.[19] The large number of reactions utilizing NADH allows *E. coli* to extract energy from diverse catabolic reactions, and the more limited number of Q8 reactions allows cells to rapidly adapt to the most prevalent terminal electron acceptor to maximize NAD^+ regeneration.

In many organisms, energy flow is mediated to varying extents by protein electron carriers (PECs), which display a wide range of sequences, structures, and cofactors (Figure 1A). Because PECs are genetically encoded, they can: (i) diversify their numbers through gene duplication,[20] (ii) tune their reduction potentials and partner specificities through mutation,[21] (iii) increase their number of redox active sites through duplication and fusion,[22] (iv) insulate electron flow by covalently coupling to partner proteins through fusion,[23] and (v) develop conformational switching that links their control over electron flow to environmental conditions.[24] An additional feature of PECs is their ability to rapidly tune their levels through mutations that alter transcription, translation, and degradation. Collectively, these features suggest that PEC duplication and specialization represents a simple way to redirect electron flow among defined sets of electron donors and acceptors. In nature, there is evidence that the expression of a non-native PEC can redirect electron flow. Cyanophages express a PEC upon infection of their host cyanobacteria that redirects electron flow as a means of increasing pigment production, photosynthesis rates, and $NADPH/NADP^+$ ratio.[25,26] This redirection of electron flow is thought to improve phage fitness by increasing the rate of deoxynucleotide biosynthesis for phage replication.[26] There is also evidence that mutations in a PEC can redirect electron flow and alter metabolite production.[27]

Genomic sequencing has revealed that the number and diversity of PECs can vary widely across species. In some cases, there may be selective pressure for specific PECs, such as evolutionary pressure for one-electron PECs that control the stepwise reduction of monooxygenases, which can produce deleterious radical oxygen species if too much electron flow occurs in the absence of a bound substrate.[28] In other cases, the underlying cause of variation in PECs is not always clear, because there is evidence that different types of PECs can support similar reactions, such as the low-potential ferredoxin (Fd) and flavodoxin (Fld) PECs that support electron transfer to an overlapping set of partner proteins.[29] During evolution, changes in the relative numbers of Fds and Flds are thought to have occurred as organisms adapted to niches with distinct nutrient availabilities. For organisms adapted to iron-limited conditions, there is evidence for an increased use of Flds and a decreased use of Fds,[29] which require iron for synthesis of their cofactor. In a comparison of other organisms, however, it is less clear why there is variation in the types of PECs that are present. In addition, PEC control over electron flow can be hard to decipher *in situ*, because we cannot reliably anticipate partner specificities and expression levels from sequence data alone. These limitations make it challenging to predict electron flow through different PECs that have the potential to relay redox in parallel or the effects of post-translational modifications on PEC coupling with partner proteins.[30,31]

IRON–SULFUR PROTEIN ELECTRON CARRIERS

One of the most intensively studied families of PECs is the Fds, which use a range of metalloclusters (2Fe2S, 3Fe4S, and 4Fe4S) to shuttle electrons.[32−34] Several lines of evidence suggest that Fds constituted a critical redox innovation during the early evolution of life.[35−38] The elements (Fe and S) in these cofactors are plentiful in hydrothermal vents that mimic the early biosphere,[35−38] Fe−S clusters spontaneously form under anaerobic environmental conditions,[39] and the highest frequencies of Fe−S binding motifs are found in methanogens, acetogens, and sulfate reducers, representing some of the earliest metabolisms to emerge.[40,41] Fds have been implicated in 18 metabolic pathways and as redox partners for proteins that catalyze >75 different reactions (Table 1).

To better understand the occurrence of Fd PECs within extant microbes, we analyzed the frequency of the smallest Fds (≤200 residues in length) having cysteine motifs that have been shown to bind 2Fe2S or 4Fe4S clusters. This size cutoff was used to enrich for single-domain PECs and minimize the inclusion of multidomain proteins that coordinate Fe−S clusters. A sampling of 92 organisms from 18 phyla (74 bacteria, 10 archaea, and 8 eukaryotes) reveals that 58% of these organisms have five or more small Fds (Figure 1B), with some organisms containing a mixture of Fd with different Fe−S cluster binding motifs. This finding suggests that Fd paralogs have evolved to function in parallel within individual microbes to allow optimal partitioning of electron flow between different partner proteins, similar to that observed in photosynthetic organisms.[42−44] However, the relative partner specificities of these small microbial Fds are still not well understood, especially in organisms whose genomes encode large numbers of family members. In addition, the relative steady-state levels of Fds have not been established for a large fraction of the family members, although there is evidence that Fds can accumulate to levels as high as 10^4−10^5 copies per cell[45,46] and vary in concentration as cells undergo the transitions between different growth phases.[47−49]

The relative efficiency by which a given Fd controls electron flow between any given set of electron donor and acceptor partner proteins depends on: (i) thermodynamic compatibility, which is determined by the relative reduction potentials of a Fd and its partner proteins, (ii) structural compatibility, which controls partner binding affinities and electron tunneling, (iii) cellular concentrations of a Fd and its partner proteins, which determine the fraction bound, and (iv) binding-induced conformational changes that influence the efficiency of electron flow. Potentiometric titrations of recombinant Fds have shown that clostridial-type Fds (typically containing two 4Fe4S clusters and capable of carrying two electrons) and plant-type Fds (containing one 2Fe2S cluster and capable of carrying one electron) are best suited for conserving energy derived from high-energy (low-potential) chemical reactions because they display the lowest potentials.[21,50] For each type of low-potential Fd, structural diversification has been observed across species (Figure 2A). This diversity has arisen during evolution through terminal extensions, loop insertions, and mutations that affect the number and types of Fe−S clusters coordinated. A comparison of Fds from a single organism, *Clostridium acetobutylicum*,[51] shows that Fd paralogs often retain the

DOI: 10.1021/acs.biochem.6b00831
Biochemistry 2016, 55, 7047−7064

Table 1. List of Fd-Partner Proteins Organized by Metabolic Pathway[a]

cellular role	Fd-partner protein (enzyme function)	source
carbon fixation	formate dehydrogenase (reductive acetyl-CoA pathway)[147]	B
	methylene-THF reductase (reductive acetyl-CoA pathway)[148]	B
	CO dehydrogenase (reductive acetyl-CoA pathway)[149,150]	BA
	formylmethanofuran oxidoreductase (reductive acetyl-CoA pathway)[151]	A
	2-ketoglutarate synthase (reverse TCA cycle)[152]	B
	pyruvate synthase (reverse TCA cycle)[152,153]	BAE
	fumarate reductase (dicarboxylate-4-hydroxybutyrate cycle)[153]	A
	succinyl-CoA reductase (dicarboxylate-4-hydroxybutyrate cycle)[153]	A
	glycine reductase (glycine synthase pathway)[154]	B
	oxalate oxidoreductase (reductive acetyl-CoA pathway)[155]	B
N and S assimilation	Fd:nitrite reductase (nitrite reduction)[156]	B
	Fd:nitrate reductase (nitrate reduction)[157]	B
	nitrogenase (N_2 fixation)[91]	B
	sulfite reductase (sulfite reduction)[158,159]	BE
photosynthesis	photosystem I (photosynthesis)[160,161]	BE
	homodimeric type I reaction center (photosynthesis)[162]	B
hydrogen metabolism	[NiFe] hydrogenase (H_2 oxidation)[163,164]	BA
	[FeFe] hydrogenase (H_2 reduction)[165]	BAE
	bifurcating hydrogenase (energy conservation)[166]	B
energy conservation	caffeoyl-CoA reductase−EtfAB complex (electron bifurcation)[167]	B
	butanoyl-CoA dehydrogenase−EtfAB complex (electron bifurcation)[168]	B
	Fd:NAD^+ reductase (Rnf) (membrane potential generation)[169,170]	B
	hydrogenase-heterodisulfide reductase (electron bifurcation)[171]	A
	NADH-dependent Fd:$NADP^+$ oxidoreductase (electron confurcation)[172]	B
	lactate dehydrogenase−EtfAB complex (electron confurcation)[173]	B
redox homeostasis	Fd:$NADP^+$ reductase (redox transfer)[174]	BE
	Fd:coenzyme F_{420} reductase (coenzyme F_{420} reduction)[175]	A
	Fd:plastoquinone reductase (cyclic electron flow)[176,177]	BE
	NADH dehydrogenase-like complex (cyclic electron flow)[178,179]	BE
	Fd:thioredoxin reductase (redox signaling)[180]	BE
glycolysis	glyceraldehyde-3-phosphate:Fd oxidoreductase (glycolysis)[181,182]	A
	pyruvate:Fd oxidoreductase (glycolysis)[183]	BAE
fermentation	acetaldehyde:Fd oxidoreductase (ethanol production)[184,185]	BA
amino acid metabolism	2-ketobutyrate synthase (synthesis and catabolism)[186]	BA
	indolepyruvate Fd oxidoreductase (catabolism)[187]	A
	2-ketoisovalerate Fd oxidoreductase (catabolism)[188]	A
	glutamate synthase (glutamate synthesis)[189,190]	BE
steroidogenesis	cytochrome p450 oxygenase (various hydroxylations)[77,191]	BE
	cholesterol side chain cleavage (hormone synthesis)[77]	E
nucleotide metabolism	xanthine dehydrogenase (purine metabolism)[192,193]	B
	ribonucleotide reductase (dNTP synthesis)[194]	B
antibiotic synthesis	mycinamicin-VIII-monooxygenase[b] (mycinamicin reduction)[195]	B
	1-deoxypentalenate monoxygenase (1-deoxypentalenate reduction)[196]	B
	pentalenolactone synthase[b] (pentalenolactone reduction)[197]	B
aromatic catabolism	anthranilate dioxygenase (anthranilate catabolism)[198]	B
	carbazole 1,9a-dioxygenase (carbazole catabolism)[199]	B
	diphenylamine dioxygenase (diphenylamine catabolism)[200]	B
	phthalate 3,4-dioxygenase (phthalate catabolism)[201]	B
	catechol 2,3-dioxygenase (catechol catabolism/enzyme repair)[202]	B
	6-hydoxynicotinate reductase (nicotinate catabolism)[203]	B
	benzoyl-CoA reductase (benzoate catabolism)[204]	B
porphyrin metabolism	heme oxygenase (phytochrome synthesis)[205]	BE
	15,16-dihydrobiliverdin:Fd oxidoreductase (phytochrome synthesis)[206]	BE
	phycoerythrobilin:Fd oxidoreductase (phytochrome synthesis)[206]	BE
	phycoerythrobilin synthase (phytochrome synthesis)[25]	V
	phytochromobilin:Fd oxidoreductase (phytochrome synthesis)[207]	BE
	phycocyanobilin:Fd oxidoreductase (phytochrome synthesis)[205]	BE
	dark protochlorophyllide oxidoreductase (chlorophyll synthesis)[208]	BE
	divinyl chlorophyllide *a* 8-vinyl-reductase (chlorophyll synthesis)[209,210]	BE
	protochlorophyllide reductase (chlorophyll synthesis)[211]	BE
	chlorophyllide *a* reductase (bacteriochlorophyll synthesis)[211]	B

DOI: 10.1021/acs.biochem.6b00831
Biochemistry 2016, 55, 7047−7064

Table 1. continued

cellular role	Fd-partner protein (enzyme function)	source
	hydroxy-chlorophyll(ide) *a* reductase (chlorophyll synthesis)[212]	E
	pheophorbide *a* oxygenase (chlorophyll degradation)[212]	E
	red chlorophyll catabolite reductase (chlorophyll degradation)[213]	E
lipid synthesis	aldehyde decarbonylase [alk(a/e)ne synthesis][214]	B
	methyl-branched lipid ω-hydroxylase[b] (lipid oxidation)[215]	B
	acyl-ACP desaturases (fatty acid desaturation)[216−218]	BE
	acyl-lipid desaturases (glycerolipid desaturation)[219−226]	BE
	acyl-ACP acetylenase (terminal alkyne synthesis)[227]	B
	geranylgeranyl reductase (membrane stabilization)[228]	A
terpenoid synthesis	4-hydroxy-3-methylbut-2-enyl-PP synthase (isoprenoid synthesis)[229,230]	BE
	4-hydroxy-3-methylbut-2-enyl-PP reductase (isoprenoid synthesis)[231]	BE
	spheroidene monooxygenase[b] (spirilloxanthin synthesis)[232]	B
	γ-glutamyl-isopropylamide hydroxylase[b] (isopropylamine degradation)[233]	B
	choline monooxygenase (osmolyte production)[234]	E
iron metabolism	pulcherriminic acid synthase (pulcherriminic acid synthesis)[235]	B
	bactrioferritin (iron mobilization)[236]	B
	cysteine desulfurase (iron−sulfur cluster biogenesis)[237,238]	BE

[a]For each partner protein, we indicate whether the partner is found in archaea (A), bacteria (B), eukaryotes (E), and viruses (V). Source annotations were based on the MetaCyc database.[146] [b]These partner proteins are all examples of Fd-dependent cytochrome P450 monooxygenases.

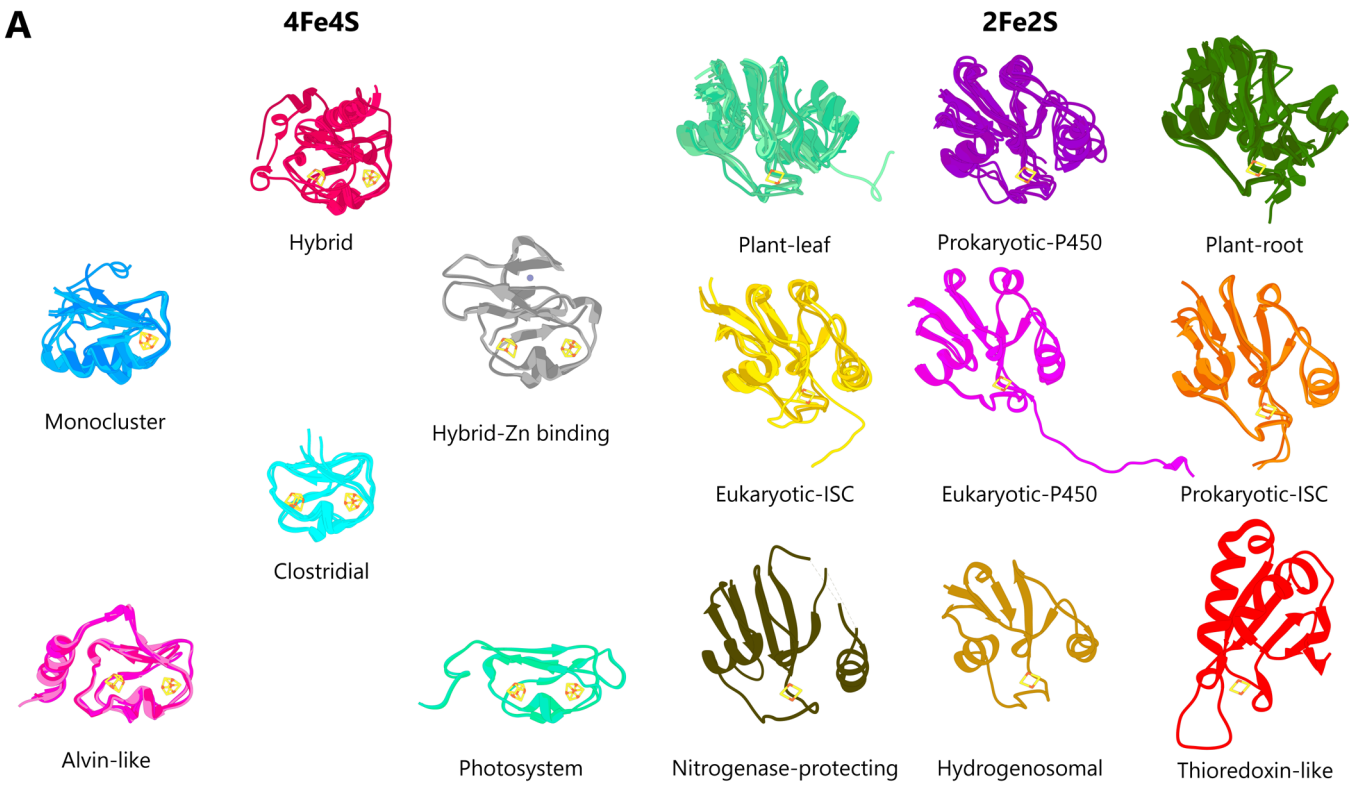

Figure 2. Ferredoxin structural diversity. (A) Comparison of 55 Fd structures reveals the structural variability that occurs within each Fd category and the structural differences between Fds from different categories. Images were generated using Chimera[143] and the PDB entries listed in Table S1. (B) Alignment of the five putative 4Fe4S Fds in *C. acetobutylicum*[51] shows how Fds that share the same cysteine motifs (yellow) within a single organism also vary in sequence because of insertions. The prolines thought to regulate stability are colored purple.[144]

cysteine residues critical for cofactor binding but vary in their sequence identity and length (Figure 2B). How this structural diversity affects the ability of different Fds to couple with the different partner proteins is not always clear, especially in microbes that contain multiple Fd paralogs and partner proteins. This issue becomes even more complex when you

DOI: 10.1021/acs.biochem.6b00831
Biochemistry 2016, 55, 7047−7064

Table 2. Categories of Small, Low-Potential Fds[a]

motif	category	cluster	PDB	$E°$ (mV)
$CX_{10-12}C_{29-34}CX_3C$	thioredoxin-like	2Fe2S	yes	not available
$CX_5CX_2CX_nC$	hydrogenosomal	2Fe2S	yes	−350[239]
	eukaryotic-P450	2Fe2S	yes	−274 to −267[240,241]
	eukaryotic-ISC	2Fe2S	yes	−353 to −342[241,242]
	prokaryotic-P450	2Fe2S	yes	−306 to −240[243,244]
	prokaryotic-ISC	2Fe2S	yes	−390 to −344[78,245]
	nitrogenase-protecting	2Fe2S	yes	−262 to −220[83,246]
	α-proteobacterial	2Fe2S	no	not available
	unclassified	2Fe2S	no	−375[79]
$CX_4CX_nCX_3C$	plant-root	2Fe2S	yes	−455 to −152[100,247]
	plant-leaf	2Fe2S	yes	−423 to −321[42,248]
$CX_2CX_nCX_3C$	clostridial	4Fe4S/4Fe4S	yes	−420 to −390[110,249]
	alvin-like	4Fe4S/4Fe4S	yes	−660 to −431[250,251]
	photosystem	4Fe4S/4Fe4S	yes	−630 to −575[252]
	nitrogenase	4Fe4S/4Fe4S	no	not available
	unclassified	4Fe4S/4Fe4S	no	−506 to −400[110]
	monocluster	4Fe4S	yes	−453 to −280[166,253]
	hybrid	4Fe4S/3Fe4S	yes	−647 to −450[102]
	hybrid-Zn binding	4Fe4S/3Fe4S	yes	−530 to −280[254]

[a]For each category, the cysteine motif and the Fe−S cluster coordinated by that motif are provided, as well as the availability of structural information in the PDB. The $CX_5CX_2CX_nC$ and $CX_4CX_nCX_3C$ motifs represent the 2Fe2S Fds that form the large cluster within the SSN shown in Figure 3; the $CX_2CX_nCX_3C$ motif represents the 4Fe4S Fds that cluster, and the $CX_{10-12}C_{29-34}CX_3C$ motif represents the 2Fe2S thioredoxin-type Fds. The midpoint potential range is also provided to illustrate the overlap between different Fd categories. The unclassified Fds represent a diverse group of proteins that do not cluster tightly with other Fd categories in the sequence similarity network and phylogenetic tree.

consider that Fd-partner proteins undergo similar diversification during evolution.

The physicochemical properties that control Fd reduction potentials and interactions with partner proteins have been extensively studied. Electrochemical studies have revealed that different Fd topologies can support a broad range of reduction potentials.[21,52] In addition, models have been developed to predict Fd reduction potentials using structural data,[53−56] which allow for analysis of their thermodynamic compatibility with different partner proteins. However, these models have been successful with only a subset of PECs, the high-potential iron−sulfur proteins,[57] and simple models that can reliably anticipate reduction potentials across all of the Fd groups have not been reported. Crystallographic studies have also provided atomic-resolution insight into the structures of many Fd and Fd-partner proteins in isolation, and mutagenesis studies have revealed the importance of Fd residues in docking to partners and electron transfer.[58] In a few cases, the molecular details of Fd and Fd-partner complexes have even been reported, including complexes made up of a Fd and Fd-NADP reductase (FNR),[59,60] Fd-thioredoxin reductase,[61] cytochromes P450 and diiron oxygenases,[62−65] Fe−Fe hydrogenase,[66] sulfite reductase,[67] and bacterioferritin.[68] These efforts have led to a detailed understanding of the residue−residue contacts that mediate binding of Fds to a small fraction of their partner proteins. This type of structural information remains challenging to generate for many partner proteins (Table 1) because of the transient nature of Fd and partner protein interactions.

SEQUENCE AND STRUCTURE RELATIONSHIPS OF FERREDOXINS

One way to study how electron flow is controlled by Fds is to study the evolutionary relationship of different Fds and their partner proteins, as well as the biophysical changes that arose in these proteins as organisms adapted to different ecological niches. Fd evolution was proposed to occur through a stepwise process whereby ancestral ISC binding peptides evolved and served as electron carriers for early energy-producing pathways;[35,69−72] peptide duplication followed by fusion led to the evolution of the smallest modern Fd,[34] and Fds with diverse energy transduction roles evolved through subsequent diversification.[72] To combat the destabilizing effects of dioxygen on 4Fe4S clusters arising from the great oxygenation event, the 2Fe2S ferredoxins are thought to have evolved,[73] which are frequently more stable in oxygen.

Three Fd topologies have been observed, which can vary in the number (one or two) and types (2Fe2S, 3Fe4S, or 4Fe4S) of metalloclusters bound. These major groups include two topologies that coordinate 2Fe2S clusters and one topology that coordinates 4Fe4S and 3Fe4S clusters. Across each Fe−S cluster type, Fds can be partitioned into additional categories (Table 2) based on structural, functional, and phylogenetic relationships. The 2Fe2S Fds have been classically differentiated into nine categories, including the plant-leaf, plant-root, hydrogenosomal, eukaryotic-P450, eukaryotic-ISC, prokaryotic-P450, prokaryotic-ISC, nitrogenase-protecting, and thioredoxin-like types.[74−87] The 4Fe4S Fds have been sorted into seven categories, including the clostridial, alvin-like, hybrid 3Fe4S/4Fe4S, hybrid-Zn binding, photosystem, nitrogenase, and monocluster types.[34,73,88−94]

To visualize how the classical Fd categories relate to one another, we generated a Fd sequence similarity network (SSN).[95] Figure 3A shows a SSN that was built by analyzing 201 Fds using the Enzyme Function Initiative-Enzyme Similarity Tool, which considers only protein sequence data.[96] The Fds used to build this network (Table S1) were primarily chosen because they had been characterized in some way, either biochemically, phylogenetically, structurally, or through interactome mapping. With this representation, each Fd is a node, connections are made between Fds having pairwise sequence identity above a

DOI: 10.1021/acs.biochem.6b00831
Biochemistry 2016, 55, 7047−7064

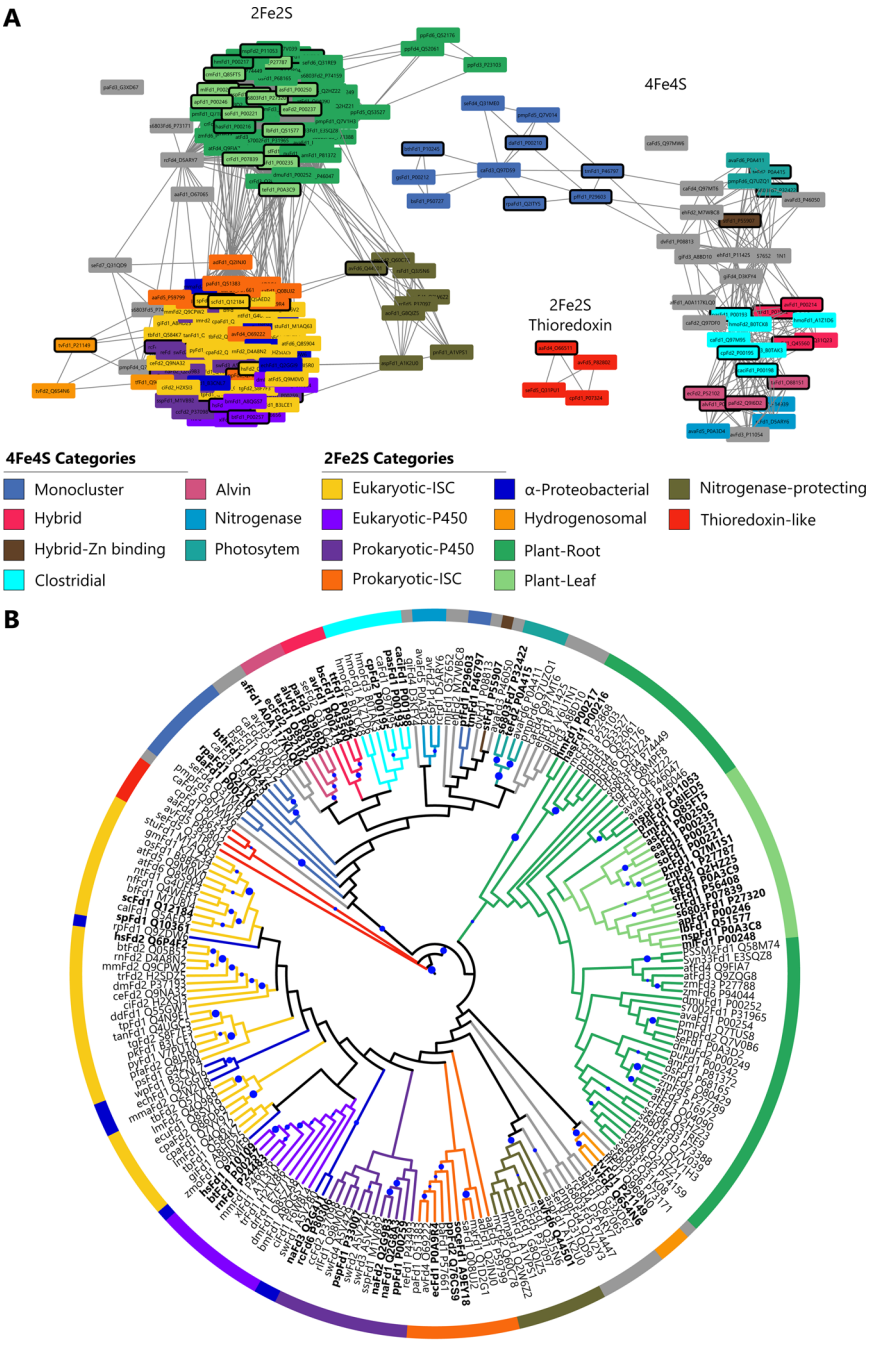

Figure 3. Ferredoxin evolutionary relationships. (A) Sequence similarity network illustrating the relationships of 201 Fd sequences. Fds are colored by category. Unclassified family members that do not cluster with previously described categories are colored gray, and Fds with determined structures are outlined in black. The network was created using the Enzyme Function Initiative-Enzyme Similarity Tool[96] and visualized using the Organic layout in Cytoscape version 3.4.[145] This network was thresholded at an alignment score of 5, including only edges greater than 5. The worst edges correspond to a median of 43.4% identity over an alignment length of 96 amino acids. (B) Phylogenetic tree built using the same Fd sequences. A structure-based multiple-sequence alignment was first generated using the MATT algorithm[97] and available structural coordinates (bold names). This alignment was then used as a rigid scaffold with the algorithm MUSCLE to map the relationships of Fd sequences lacking structures.[98] Gaps were added to sequences lacking structures to identify their best placement. Maximal parsimony UPGMA clustering was applied to the expanded MSA to create a structure-anchored phylogenetic tree. Bootstrap percentages out of 100 trees are represented as blue circles ranging in size representing 50−100% confidence.

threshold, and clusters arise on the basis of the number and strength of connections formed between Fds.[96] This representation illustrates clear demarcations between several of the Fd categories. The 2Fe2S, 4Fe4S, and thioredoxin-like Fds fall into three major clusters that contain subclusters corresponding to the 16 classical Fd categories. In addition, there are Fds that do not clearly cluster with these classical 16 groups, including many unclassified Fds with 2Fe2S or 4Fe4S cluster motifs. The weak connectivity of these unclassified Fds can be more readily visualized by using a higher-alignment score thresholding value (Figure S1). Within the SSN, there is also a group that we designate the α-proteobacterial Fds that cluster with the P450-type and ISC-type Fds but do not appear to not clearly segregate with either group.

DOI: 10.1021/acs.biochem.6b00831
Biochemistry 2016, 55, 7047−7064

One benefit of the two-dimensional SSN representation is that it displays subtle connections between different Fds that can be hard to identify using a phylogenetic tree. For example, the SSN shows that a majority of the 2Fe2S Fds fall into two dense subclusters. The first major cluster includes the plant-root and plant-leaf Fd categories, while the second dense cluster includes the ISC, P450, and α-proteobacterial Fd categories. On the periphery of these dense clusters of tightly connected Fds are smaller clusters. Some of these smaller clusters display weak connectivity to one or both of the major clusters. For example, the hydrogenosomal Fd category is weakly connected to the dense ISC/P450 cluster. The nitrogenase-protecting Fd category, in contrast, shows connectivity to both dense clusters. An additional benefit of the SSN is that it reveals how the state of our Fd structural knowledge relates to sequence diversity. Some categories such as plant-leaf Fds have had many structures reported across their subcluster within the SSN, while others such as eukaryotic-ISC, prokaryotic-ISC, nitrogenase, and nitrogenase-protecting have been more sparsely sampled. Even among the plant-root Fds, there is a subset of family members that are only weakly connected to the major cluster that lack structural information. These are bacterial Fds that interact with dioxygenases.

To evaluate how the different Fds relate to one another, we also generated a phylogenetic tree (Figure 3B). This tree was built by combining structural[97] and sequence[98] alignment techniques to relate Fds with high levels of sequence diversity. The tree reveals a clear demarcation of the three major clusters observed in the SSN, which represent the 2Fe2S, 4Fe4S, and thioredoxin-like Fd topologies. This tree also exposes overlaps between several of the Fd categories. Proximal to the P450-type 2Fe2S groups (prokaryotic and eukaryotic) are the α-proteobacterial Fds, which are from organisms that are closely related to the endosymbionts that formed the mitochondria. In addition, the tree shows a number of additional Fds that do not fall into the classical categories, whose branch tips are colored gray. Many of these unclassified Fds are located at the junction between different Fd categories and have small confidence values, for example, between the nitrogenase-protecting and hydrogenosomal Fds as well as between the photosystem and plant Fds.

Our phylogenetic analyses suggest areas where the Fd family would benefit from additional structural investigation. Protein structures have been reported for a majority of the classical Fd categories, with the exception of the nitrogenase-type (4Fe4S) and the α-proteobacterial (2Fe2S) Fds, whose topologies might provide insight into their relationship with the eukaryotic and prokaryotic ISC and P450 Fds. Our tree also illustrates why there is a need to understand the structure and functions of the unclassified Fds, which appear at junctions between clusters in the SSN. Examples of unclassified Fds include *Aquifex aeolicus* Fd1 (O67065), *Rhodobacter capsulatus* Fd4 (D5ARY7), and *C. acetobutylicum* Fd2 (Q97DF0). The lack of structural information for these proteins limits our ability to use structure-based models to anticipate their thermodynamic compatibility with potential partner proteins.[53−56]

THE CHALLENGE OF PREDICTING FD FUNCTIONS

Although it is straightforward to relate newly discovered Fds to existing categories through sequence relationships, their physical properties do not always segregate across the different Fd categories, which limits our ability to predict their *in situ* control of electron flow by studying their evolutionary relationships to characterized Fds. For example, measurements of reduction potentials across different Fd groups have revealed overlapping values (Table 2). In *Arabidopsis thaliana*, which contains four 2Fe2S plant Fds,[99] the Fd midpoint potentials range from −152 mV (atFd4, Q9FIA7) to −433 mV (atFd2, P16972).[100,101] Studies of 4Fe4S Fds have also revealed wide-ranging reduction potentials, from −280 to −650 mV,[21,102] which overlap with a subset of potentials observed in the plant Fds. The full range of reduction potential across each Fd category has not been established, and our ability to use protein Langevin dipole calculations to estimate midpoint potentials[53−56] remains limited. Further studies are needed to determine the full range of reduction potentials that can exist within each Fd category, and models that can anticipate midpoint potentials across all Fd groups are needed.

Biochemical studies have also revealed that Fd-partner specificity can vary across a Fd category in a single organism, which emphasizes the need to develop sequence−structure−function insight that predicts electron flow through colocalized Fds. This challenge is best illustrated by Fd studies in photosynthetic organisms. Interactome studies examining the proteome-wide specificity of the six plant-type Fd paralogs in the single-cell alga *Chlamydomonas reinhardtii* revealed a range of specialization for these proteins, which all colocalize to the chloroplast under normal growth conditions.[42,43] Some of these Fds display orthogonal partner specificity, binding to completely different sets of partner proteins, while others display distinct but overlapping partner specificity profiles.[42,43] Cellular and genetic studies in cyanobacteria have also revealed a range of Fd-partner specificities.[44] For example, *Synechocystis* sp. PCC 6803 contains nine Fds from three groups (four plant-type, two bacterial type, and three 4Fe4S), while *Anabaena variabilis* has a mixture of plant-type and 4Fe4S-nitrogenase Fds.[44] In addition, analysis of the four plant-type Fds in *A. thaliana* revealed diverse partner specificities, with patterns of specificity similar to those of *C. reinhardtii*.[100,101,103,104] *A. thaliana* also has colocalized eukaryotic-P450 and eukaryotic-ISC Fds within their mitochondria whose specificities have not been well established.[81]

Interactomes have not yet been reported for nonphotosynthetic microbes, which can contain large numbers of small proteins with Fe−S binding motifs (Figure 1B), although there have been detailed molecular studies of numerous Fds and Fd-partner proteins. These latter efforts have provided evidence that partner specificity can vary across Fds, with some Fds efficiently delivering electrons to many acceptor proteins, even noncognate partner proteins, and others appearing more restricted in their coupling.[101,105−111] In the case of the prokaryotic P450-type Fd (putidaredoxin, ppFd1, P00259), which reduces P450cam,[106] structural studies have suggested a mechanism for specificity with P450cam. Binding of putidaredoxin to P450cam induces a conformational change that increases the access of bulk solvent to the active site.[106] Fd conformational switching can also regulate partner binding. For example, the nitrogenase-protecting Fd from *Azotobacter vinelandii* (AvFd6, Q44501) undergoes a major conformational shift upon oxidation, which triggers it to bind and inactivate nitrogenase, yielding protection from dioxygen.[24] Taken together, these findings suggest that some Fds achieve specificity for partner proteins by evolving inter- and intramolecular interactions that allow for allosteric regulation of electron flow.

DOI: 10.1021/acs.biochem.6b00831
Biochemistry 2016, 55, 7047−7064

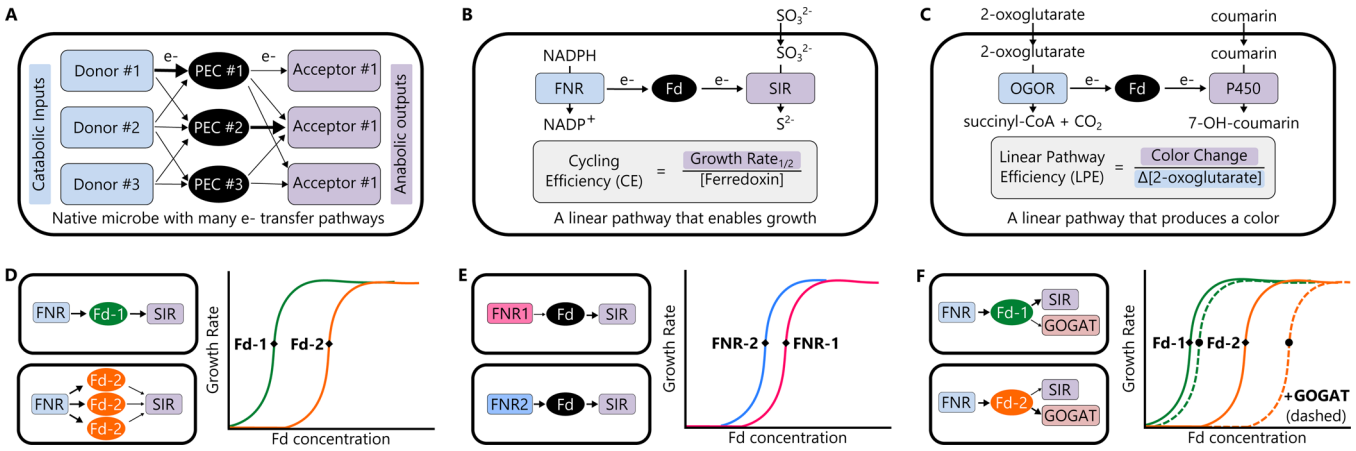

Figure 4. Cellular assays for analyzing ferredoxin control over electron flow. (A) In cells with multiple Fds and Fd-partner proteins, it is challenging to determine how each Fd controls electron flow between the various donor and acceptor proteins. (B) In contrast, electron flow mediated by a single Fd can be analyzed in cells using a selection. Selections for Fd yield cell growth only when the Fd shuttles electrons to an acceptor protein whose activity complements the defect of a bacterial auxotroph, such as a sulfide auxotroph that requires a Fd-dependent sulfite reductase (SIR) to grow on a medium containing sulfate as the sulfur source.[111] A simple parameter for quantifying Fd control over electron flow in a selection is cycling efficiency (CE), defined as the half-maximal growth rate observed over a range of Fd concentrations normalized to the Fd concentration that yields half-maximal growth. (C) A screen for Fd electron transfer activity generates a measurable color output by using the Fd-dependent activity of an oxygenase to convert a substrate to a colored product that can be visualized. Examples of substrates that can be used to report on oxygenase activities in whole cells include biphenyl, dibenzofuran, toluene, 4-picoline, and benzylpyrrolidine.[113,114,119] In screens and selections, the acceptor/donor protein activity ratio, e.g., the ratio of the color intensity generated by an acceptor protein to the consumption of the substrate by the donor protein, can be used to calculate the efficiency of a three-component pathway over a range of growth and expression conditions. (D) When different Fds are compared using a selection with the same donor and acceptor proteins, their CEs are expected to vary as illustrated with diamonds requiring differential expression to achieve equivalent electron flow. (E) In cellular assays, one of the Fd-partner proteins can also be varied to study sequence−structure−function relationships. (F) The specificity of a given Fd for a pair of partner proteins can be assayed using a selection by comparing the CE of a Fd in the presence of one partner acceptor partner (diamond) vs two partner proteins (circle).

CELLULAR APPROACHES FOR ANALYZING FDS

Hard-won physical data generated using purified Fds provides detailed insight into their physicochemical properties and ability to deliver electrons to specific partner proteins in isolation. However, biophysical studies alone are limited in their ability to estimate Fd control over electron flow to a given partner protein under the complex conditions within cells where Fds interact with multiple donor and acceptor proteins and are subject to competing reactions that can cause leakage of electrons from a given energy transduction pathway. *In vitro* biochemical studies are also limited in their ability to estimate the percentage of reduced Fds that shuttle electrons between their partner proteins (pathway efficiency) versus off-pathway chemical reactions (electron leakage) *in situ*. Furthermore, *in vitro* studies are inherently limited by the rate at which they can generate biochemical data on partner specificity for large numbers of Fds, whose numbers have exploded with genomic data, and their ability to anticipate how Fds function in synthetic electron transfer pathways.

To improve our understanding of Fd sequence−function relationships, we propose a new concept. Efforts should be made to measure and compare how divergent Fds mediate electron transfer between defined sets of partner proteins within the context of the cellular milieu. Specifically, we propose measuring how Fds with similar reduction potentials differ in their ability to support energy flow through simple electron transfer pathways when present at identical cellular concentrations. Currently, this type of measurement is hard to make because cells often express multiple PECs and partner proteins in parallel (Figure 4A), whose individual contributions to electron flow can be hard to quantify. To allow cellular analysis of Fd, we propose creating cells with a minimal set of PECs and partner proteins and introducing electron transfer pathways into these strains that generate an easy-to-measure output when a given Fd transfers electrons between a pair of donor and acceptor proteins (Figure 4B,C). To quantify and compare Fd control over electron flow in these cellular assays, electron donor and acceptor proteins with activities that can be easily monitored must be chosen. In addition, Fd expression will need to be placed under control of a ligand-inducible promoter so that cellular measurements can be performed with Fds expressed at different steady-state levels. These aspects of the proposed assays will allow for calculations of linear pathway efficiency (LPE), defined as the ratio of acceptor/donor oxidoreductase activities. Fd and partner protein concentrations are expected to affect the flux through pathways, i.e., output per cell per time. To allow for comparisons of divergent Fds in a given pathway, we propose calculating the coupling efficiency (CE) of ferredoxins, defined as the half-maximal activity through the pathway when donors and acceptors are constitutively expressed normalized to the Fd concentration that yields half-maximal activity. In cases in which a Fd couples well with a given pair of donor and acceptor proteins, then CE will be large because a low Fd concentration should yield half-maximal activity through the pathway (Figure 4D). In contrast, a Fd that couples poorly to the same pair of partner proteins will require a higher cellular concentration for half-maximal activity and will display a smaller CE. Provided that the Fds being compared have similar midpoint potentials, Fds are expected to yield a similar maximal output in cellular assays. This approach should also be useful for comparing the activity of Fd-partner protein homologues with divergent sequences (Figure 4E).

Fd-dependent cellular assays have been reported, although these assays have not yet been used to quantify how divergent

DOI: 10.1021/acs.biochem.6b00831
Biochemistry 2016, 55, 7047−7064

Fds differ in their cellular behaviors. The first cellular assays to incorporate Fds were aerobic screens for oxygenases, tripartite systems typically consisting of a FNR electron donor, a Fd, and either a cytochrome P450 monooxygenase or a dioxygenase acceptor.[112−119] With some of these cellular assays, Fd-dependent oxygenase activity can be measured through colorimetric detection of the product,[113,114,117,119] a strategy that is compatible with high-throughput screening. More recently, a cellular assay was described that can be used to select for Fds that shuttle electrons between a donor and acceptor protein in *E. coli*. For this assay, an *E. coli* sulfide auxotroph was built by deleting the gene encoding sulfite reductase (SIR), an NADPH-dependent enzyme, such that the strain could no longer grow on minimal medium that contains sulfate as the only sulfur source.[111,120] The growth defect could be complemented by a tripartite system that consists of a Fd electron donor (FNR), a Fd, and a Fd-dependent SIR from plants. Unlike the Fd-dependent oxygenase screens, which require aerobic conditions to analyze Fds,[112−119] this sulfide auxotroph is compatible with Fd analysis under both aerobic and anaerobic conditions.[111]

Because Fds support biological reactions that are often essential for growth (amino acid biosynthesis, nitrogen assimilation, C and N fixation, glycolysis, and respiration), we posit that additional growth selections for Fd activity can be built by deleting different genes encoding essential metabolic enzymes in bacteria and rescuing cellular growth defects by expressing Fd-dependent partner proteins (Table 1). There are several challenges to diversifying cellular selections for Fds. First, genes encoding oxidoreductases must be chromosomally disrupted to create microbial strains that have specialized nutrient requirements. Second, non-native Fd-dependent oxidoreductases need to be expressed as functional enzymes in these mutant strains. In some cases, these challenges may be straightforward to overcome. For example, an *E. coli* glutamate auxotroph could be created by replacing the native NADPH-dependent glutamate synthase with a Fd-dependent glutamine oxoglutarate aminotransferase (GOGAT), which are found in plants and cyanobacteria.[121] In fact, *Synechocystis* sp. PCC 6803 GOGAT has been previously expressed as a functional protein within *E. coli*,[121] suggesting that this GOGAT could be used to rescue the growth defects in an *E. coli* strain having mutations in the native glutamate synthase. With other Fd acceptor proteins, it may be more challenging to build cellular assays that report on their coupling to Fds. This challenge could arise with Fd-dependent oxidoreductases that require specialized protein machinery for cofactor maturation that is not present in non-native hosts, such as CO dehydrogenases and nitrogenases.

We posit that a range of cellular assays can be developed for studying Fds in cells. These approaches should be useful for measuring: (i) how Fds with divergent sequences differ in their LPE and CE, (ii) how much CE can vary among Fds with similar reduction potentials but divergent sequences, and (iii) how cellular growth conditions affect LPE and CE. To quantify CEs of various PECs, the product of the three-component, linear electron transfer pathway will need to be measured, i.e., the colorimetric changes or growth rates of the cells, and these values will need to be normalized to the concentration of holo-Fd in cells, which could be analyzed by measuring the amplitudes of the signature spectra of the 2Fe2S- and 4Fe4S-type Fd in cellular lysates.[122−124] The LPE of synthetic pathways could also be determined in cases in which the input and output of the linear pathway can be quantified. Measurements of electron inputs into three-component pathways will necessitate the use of analytical methods that examine time-dependent changes in the substrate being used as an electron source. When electrons are derived from a chemical that is provided at defined concentrations within growth medium, e.g., by using 2-oxoglutarate:Fd oxidoreductase (OGOR) and 2-oxoglutarate as a source of electrons,[125] changes in the concentration of that chemical can be used to estimate the electron flow into the donor. The values obtained from electron input and output can then be combined to calculate LPE.

Fd cycling efficiency is expected to vary with the linear redox pathway being studied. In theory, all of the electrons used to reduce a given Fd could be used by the Fd to reduce an acceptor protein such that LPE approaches a value of 1. However, Fds often participate in transient interactions with partner proteins, and losses are expected to arise from off-target pathway oxidation arising from dioxygen reduction. Addition of branches to linear pathways could be useful for studying partitioning of electron flow to a set of electron acceptors. By analyzing CE and LPE through pathways having one or more competing electron acceptor proteins, cellular assays can be used to quantify the proportion of electrons that flow to different partner proteins within a cellular context. For example, the linear pathway shown in Figure 4B could be used to analyze Fd control over electron flow in the presence and absence of a second electron acceptor protein like GOGAT (Figure 4F). In cases in which a Fd couples strongly to SIR but not to GOGAT, the Fd concentration required for half-maximal complementation will be similar in the absence and presence of GOGAT. However, in cases in which a Fd couples more strongly to GOGAT than SIR, the Fd concentration required for half-maximal growth will increase in the presence of GOGAT, provided that Fd-partner proteins are expressed at levels that allow for detection of their differences in affinities.

By studying CE and LPE, we posit that insight can be gleaned that will allow us to begin anticipating the proportion of electrons that different Fds can deliver across the Fd interactome in natural and engineered microbes. The strategy outlined for studying Fd sequence−structure−function relationships should be applicable to other families of PECs, like flavodoxins, because these PECs can display low reduction potentials and substitute for Fds in electron shuttling.[29,126−128] Understanding the functional overlap and competition between Flds and various Fds in particular cell reactions and circumstances could yield a more global appreciation of the contributions of specific PECs in cellular electron fluxes. In addition, assays that report on PEC cycling efficiencies can be used to compare the time-dependent characteristics of Fds and Flds (e.g., lifetimes, stabilities to oxidants, and degradation) by producing PECs for a defined period of time and assessing their coupling to partner proteins after stopping their synthesis.

SYNTHETIC ENERGY-CONSERVING PATHWAYS

Our ability to control the expression of metabolic enzymes and carbon flux is poised to make great strides as our ability to design regulatory networks continues to improve, with tools now available for microbial design automation.[129] Redox synthetic biology, in contrast, faces a major bottleneck, namely our inability to anticipate or optimize electron flow between redox proteins within microbes and the effects of introducing non-natural proteins on redox homeostasis. This bottleneck will continue to impede our ability to construct energy-conserving pathways in cells that prevent global redox imbalances, which can be a significant problem in certain metabolic engineering

DOI: 10.1021/acs.biochem.6b00831
Biochemistry 2016, 55, 7047−7064

applications. While there have been reports of successful construction of non-native electron transfer pathways in cells,[111,130−136] as well as visual probes for 2Fe2S clusters and PEC reduction states,[137−140] our understanding of electron flow mediated by PECs remains more limited. We propose that the cellular assays described herein will be useful for providing a more quantitative, comprehensive approach for future electron flow design efforts. By identifying Fd and Fd-partner pairs that insulate electron flow from the natural redox machinery in cells (orthogonal redox proteins), researchers can identify biological parts that can be used to rationally optimize existing energy-conserving pathways to maximize product yields. Additionally, the identification of mutations that alter the proportion of electrons that a given Fd delivers to its native partner proteins could be used to improve product yields, as has been reported for *C. reinhardtii* Fd, which yields improved H_2 photoproduction rates when mutations that alter electron proportioning to FNR and hydrogenase are incorporated.[27] The sites targeted for mutations in this previous study were identified by examining the nuclear magnetic resonance chemical shift perturbation of a Fd upon complex formation with each partner protein, a low-throughput approach, and identifying residues that are uniquely important to the interaction with one partner.[27] Improvements in metabolic yields could also be achieved by using Fds in synthetic extracellular electron transfer pathways[141] or by implementing Fds in metabolic transistor-like control processes, which have been shown to permit fine control over metabolic fluxes.[16] By extending these studies from Fds to other PECs, such as Flds, we can begin to develop rules for understanding what controls the proportion of electrons that are transferred between different metabolic pathways and derive improved electron-flux maps (electron fluxome).

■ ASSOCIATED CONTENT

Supporting Information

The Supporting Information is available free of charge on the ACS Publications website at DOI: 10.1021/acs.biochem.6b00831.

One supplementary figure (PDF)

One supplementary table (XLSX)

■ AUTHOR INFORMATION

Corresponding Author

*Department of Biosciences, Rice University, 6100 Main St., Houston, TX 77005. Telephone: 713-348-3849. Email: joff@rice.edu.

ORCID

Jonathan J. Silberg: 0000-0001-5612-0667

Funding

This work was supported by U.S. Department of Energy Grant DE-SC0014462 (to G.N.B. and J.J.S.). J.T.A. was supported by the National Science Foundation Graduate Research Fellowship Program (NSF GFRP) under Grant R3E821.

Notes

The authors declare no competing financial interest.

■ ACKNOWLEDGMENTS

We are grateful to Patsy Babbitt for helpful discussions as we generated the SSN.

■ ABBREVIATIONS

CE, cycling efficiency; Fd, ferredoxin; Fld, flavodoxin; FNR, Fd:NADP reductase; GOGAT, glutamine oxoglutarate aminotransferase; LPE, linear pathway efficiency; PDB, Protein Data Bank; PEC, protein electron carrier; SSN, sequence similarity network; SIR, sulfite reductase

■ REFERENCES

(1) Kochanowski, K., Sauer, U., and Noor, E. (2015) Posttranslational regulation of microbial metabolism. *Curr. Opin. Microbiol. 27*, 10−17.

(2) Olson, E. J., and Tabor, J. J. (2012) Post-translational tools expand the scope of synthetic biology. *Curr. Opin. Chem. Biol. 16*, 300−306.

(3) Russell, J. B., and Cook, G. M. (1995) Energetics of bacterial growth: balance of anabolic and catabolic reactions. *Microbiol. Rev. 59*, 48−62.

(4) Holtz, W. J., and Keasling, J. D. (2010) Engineering static and dynamic control of synthetic pathways. *Cell 140*, 19−23.

(5) Kobayashi, H., Kaern, M., Araki, M., Chung, K., Gardner, T. S., Cantor, C. R., and Collins, J. J. (2004) Programmable cells: interfacing natural and engineered gene networks. *Proc. Natl. Acad. Sci. U. S. A. 101*, 8414−8419.

(6) Solomon, K. V., Sanders, T. M., and Prather, K. L. J. (2012) A dynamic metabolite valve for the control of central carbon metabolism. *Metab. Eng. 14*, 661−671.

(7) Liu, D., Xiao, Y., Evans, B. S., and Zhang, F. (2015) Negative feedback regulation of fatty acid production based on a malonyl-CoA sensor-actuator. *ACS Synth. Biol. 4*, 132−140.

(8) Cross, P. J., Allison, T. M., Dobson, R. C. J., Jameson, G. B., and Parker, E. J. (2013) Engineering allosteric control to an unregulated enzyme by transfer of a regulatory domain. *Proc. Natl. Acad. Sci. U. S. A. 110*, 2111−2116.

(9) Dietrich, J. A., Shis, D. L., Alikhani, A., and Keasling, J. D. (2013) Transcription factor-based screens and synthetic selections for microbial small-molecule biosynthesis. *ACS Synth. Biol. 2*, 47−58.

(10) Dueber, J. E., Wu, G. C., Malmirchegini, G. R., Moon, T. S., Petzold, C. J., Ullal, A. V., Prather, K. L. J., and Keasling, J. D. (2009) Synthetic protein scaffolds provide modular control over metabolic flux. *Nat. Biotechnol. 27*, 753−759.

(11) Delebecque, C. J., Lindner, A. B., Silver, P. A., and Aldaye, F. A. (2011) Organization of intracellular reactions with rationally designed RNA assemblies. *Science 333*, 470−474.

(12) Conrado, R. J., Wu, G. C., Boock, J. T., Xu, H., Chen, S. Y., Lebar, T., Turnšek, J., Tomšič, N., Avbelj, M., Gaber, R., Koprivnjak, T., Mori, J., Glavnik, V., Vovk, I., Benčina, M., Hodnik, V., Anderluh, G., Dueber, J. E., Jerala, R., and DeLisa, M. P. (2012) DNA-guided assembly of biosynthetic pathways promotes improved catalytic efficiency. *Nucleic Acids Res. 40*, 1879−1889.

(13) Chen, A. H., Robinson-Mosher, A., Savage, D. F., Silver, P. A., and Polka, J. K. (2013) The bacterial carbon-fixing organelle is formed by shell envelopment of preassembled cargo. *PLoS One 8*, e76127.

(14) Guntas, G., Mitchell, S. F., and Ostermeier, M. (2004) A molecular switch created by *in vitro* recombination of nonhomologous genes. *Chem. Biol. 11*, 1483−1487.

(15) Taylor, N. D., Garruss, A. S., Moretti, R., Chan, S., Arbing, M. A., Cascio, D., Rogers, J. K., Isaacs, F. J., Kosuri, S., Baker, D., Fields, S., Church, G. M., and Raman, S. (2015) Engineering an allosteric transcription factor to respond to new ligands. *Nat. Methods 13*, 177−183.

(16) Wu, H., Tuli, L., Bennett, G. N., and San, K.-Y. (2015) Metabolic transistor strategy for controlling electron transfer chain activity in *Escherichia coli*. *Metab. Eng. 28*, 159−168.

(17) Sánchez, A. M., Andrews, J., Hussein, I., Bennett, G. N., and San, K.-Y. (2006) Effect of overexpression of a soluble pyridine nucleotide transhydrogenase (UdhA) on the production of poly(3-hydroxybutyrate) in *Escherichia coli*. *Biotechnol. Prog. 22*, 420−425.

DOI: 10.1021/acs.biochem.6b00831
Biochemistry 2016, 55, 7047−7064

(18) Sánchez, A. M., Bennett, G. N., and San, K.-Y. (2005) Effect of different levels of NADH availability on metabolic fluxes of *Escherichia coli* chemostat cultures in defined medium. *J. Biotechnol. 117*, 395−405.
(19) Orth, J. D., Conrad, T. M., Na, J., Lerman, J. A., Nam, H., Feist, A. M., and Palsson, B. Ø. (2011) A comprehensive genome-scale reconstruction of *Escherichia coli* metabolism–2011. *Mol. Syst. Biol. 7*, 535.
(20) George, D. G., Hunt, L. T., Yeh, L. S., and Barker, W. C. (1985) New perspectives on bacterial ferredoxin evolution. *J. Mol. Evol. 22*, 20−31.
(21) Battistuzzi, G., D'Onofrio, M., Borsari, M., Sola, M., Macedo, A. L., Moura, J. J., and Rodrigues, P. (2000) Redox thermodynamics of low-potential iron-sulfur proteins. *JBIC, J. Biol. Inorg. Chem. 5*, 748−760.
(22) Reeve, J. N., Beckler, G. S., Cram, D. S., Hamilton, P. T., Brown, J. W., Krzycki, J. A., Kolodziej, A. F., Alex, L., Orme-Johnson, W. H., and Walsh, C. T. (1989) A hydrogenase-linked gene in *Methanobacterium thermoautotrophicum* strain delta H encodes a polyferredoxin. *Proc. Natl. Acad. Sci. U. S. A. 86*, 3031−3035.
(23) Yacoby, I., Pochekailov, S., Toporik, H., Ghirardi, M. L., King, P. W., and Zhang, S. (2011) Photosynthetic electron partitioning between [FeFe]-hydrogenase and ferredoxin:NADP+-oxidoreductase (FNR) enzymes *in vitro*. *Proc. Natl. Acad. Sci. U. S. A. 108*, 9396−9401.
(24) Schlesier, J., Rohde, M., Gerhardt, S., and Einsle, O. (2016) A Conformational Switch Triggers Nitrogenase Protection from Oxygen Damage by Shethna Protein II (FeSII). *J. Am. Chem. Soc. 138*, 239−247.
(25) Dammeyer, T., Bagby, S. C., Sullivan, M. B., Chisholm, S. W., and Frankenberg-Dinkel, N. (2008) Efficient phage-mediated pigment biosynthesis in oceanic cyanobacteria. *Curr. Biol. 18*, 442−448.
(26) Thompson, L. R., Zeng, Q., Kelly, L., Huang, K. H., Singer, A. U., Stubbe, J., and Chisholm, S. W. (2011) Phage auxiliary metabolic genes and the redirection of cyanobacterial host carbon metabolism. *Proc. Natl. Acad. Sci. U. S. A. 108*, E757−64.
(27) Rumpel, S., Siebel, J. F., Farès, C., Duan, J., Reijerse, E., Happe, T., Lubitz, W., and Winkler, M. (2014) Enhancing hydrogen production of microalgae by redirecting electrons from photosystem I to hydrogenase. *Energy Environ. Sci. 7*, 3296−3301.
(28) Munro, A. W., Girvan, H. M., and McLean, K. J. (2007) Cytochrome P450–redox partner fusion enzymes. *Biochim. Biophys. Acta, Gen. Subj. 1770*, 345−359.
(29) Pierella Karlusich, J. J., Lodeyro, A. F., and Carrillo, N. (2014) The long goodbye: the rise and fall of flavodoxin during plant evolution. *J. Exp. Bot. 65*, 5161−5178.
(30) Wu, X., Vellaichamy, A., Wang, D., Zamdborg, L., Kelleher, N. L., Huber, S. C., and Zhao, Y. (2013) Differential lysine acetylation profiles of *Erwinia amylovora* strains revealed by proteomics. *J. Proteomics 79*, 60−71.
(31) Mo, R., Yang, M., Chen, Z., Cheng, Z., Yi, X., Li, C., He, C., Xiong, Q., Chen, H., Wang, Q., and Ge, F. (2015) Acetylome analysis reveals the involvement of lysine acetylation in photosynthesis and carbon metabolism in the model cyanobacterium *Synechocystis sp.* PCC 6803. *J. Proteome Res. 14*, 1275−1286.
(32) Beinert, H., Holm, R. H., and Münck, E. (1997) Iron-sulfur clusters: nature's modular, multipurpose structures. *Science 277*, 653−659.
(33) Fontecave, M. (2006) Iron-sulfur clusters: ever-expanding roles. *Nat. Chem. Biol. 2*, 171−174.
(34) Meyer, J. (2008) Iron-sulfur protein folds, iron-sulfur chemistry, and evolution. *JBIC, J. Biol. Inorg. Chem. 13*, 157−170.
(35) Wächtershäuser, G. (2006) From volcanic origins of chemoautotrophic life to Bacteria, Archaea and Eukarya. *Philos. Trans. R. Soc., B 361*, 1787−1806 , discussion 1806−1808.
(36) Wächtershäuser, G. (1988) Before enzymes and templates: theory of surface metabolism. *Microbiol. Rev. 52*, 452−484.
(37) Wächtershäuser, G. (1992) Groundworks for an evolutionary biochemistry: the iron-sulphur world. *Prog. Biophys. Mol. Biol. 58*, 85−201.
(38) Hazen, R. M., and Sverjensky, D. A. (2010) Mineral surfaces, geochemical complexities, and the origins of life. *Cold Spring Harbor Perspect. Biol. 2*, a002162.
(39) Malkin, R., and Rabinowitz, J. C. (1966) The reconstitution of clostridial ferredoxin. *Biochem. Biophys. Res. Commun. 23*, 822−827.
(40) Sousa, F. L., Thiergart, T., Landan, G., Nelson-Sathi, S., Pereira, I. A. C., Allen, J. F., Lane, N., and Martin, W. F. (2013) Early bioenergetic evolution. *Philos. Trans. R. Soc., B 368*, 20130088.
(41) Ramos, A. R., Keller, K. L., Wall, J. D., and Pereira, I. A. C. (2012) The Membrane QmoABC Complex Interacts Directly with the Dissimilatory Adenosine 5′-Phosphosulfate Reductase in Sulfate Reducing Bacteria. *Front. Microbiol. 3*, 137.
(42) Terauchi, A. M., Lu, S.-F., Zaffagnini, M., Tappa, S., Hirasawa, M., Tripathy, J. N., Knaff, D. B., Farmer, P. J., Lemaire, S. D., Hase, T., and Merchant, S. S. (2009) Pattern of expression and substrate specificity of chloroplast ferredoxins from *Chlamydomonas reinhardtii*. *J. Biol. Chem. 284*, 25867−25878.
(43) Peden, E. A., Boehm, M., Mulder, D. W., Davis, R., Old, W. M., King, P. W., Ghirardi, M. L., and Dubini, A. (2013) Identification of global ferredoxin interaction networks in *Chlamydomonas reinhardtii*. *J. Biol. Chem. 288*, 35192−35209.
(44) Cassier-Chauvat, C., and Chauvat, F. (2014) Function and Regulation of Ferredoxins in the Cyanobacterium, *Synechocystis* PCC6803: Recent Advances. *Life (Basel, Switz.) 4*, 666−680.
(45) Doucette, G. J., Erdner, D. L., Peleato, M. L., Hartman, J. J., and Anderson, D. M. (1996) Quantitative analysis of iron-stress related proteins in *Thalassiosira weissflogii*: measurement of flavodoxin and ferredoxin using HPLC. *Mar. Ecol.: Prog. Ser. 130*, 269−276.
(46) Soufi, B., Krug, K., Harst, A., and Macek, B. (2015) Characterization of the *Escherichia coli* proteome and its modifications during growth and ethanol stress. *Front. Microbiol. 6*, 103.
(47) Rydzak, T., McQueen, P. D., Krokhin, O. V., Spicer, V., Ezzati, P., Dwivedi, R. C., Shamshurin, D., Levin, D. B., Wilkins, J. A., and Sparling, R. (2012) Proteomic analysis of *Clostridium thermocellum* core metabolism: relative protein expression profiles and growth phase-dependent changes in protein expression. *BMC Microbiol. 12*, 214.
(48) Zhang, W., Gritsenko, M. A., Moore, R. J., Culley, D. E., Nie, L., Petritis, K., Strittmatter, E. F., Camp, D. G., Smith, R. D., and Brockman, F. J. (2006) A proteomic view of *Desulfovibrio vulgaris* metabolism as determined by liquid chromatography coupled with tandem mass spectrometry. *Proteomics 6*, 4286−4299.
(49) Wang, S. P., Kang, P. J., Chen, Y. P., and Ely, B. (1995) Synthesis of the Caulobacter ferredoxin protein, FdxA, is cell cycle controlled. *J. Bacteriol. 177*, 2901−2907.
(50) Liu, J., Chakraborty, S., Hosseinzadeh, P., Yu, Y., Tian, S., Petrik, I., Bhagi, A., and Lu, Y. (2014) Metalloproteins containing cytochrome, iron-sulfur, or copper redox centers. *Chem. Rev. 114*, 4366−4469.
(51) Nölling, J., Breton, G., Omelchenko, M. V., Makarova, K. S., Zeng, Q., Gibson, R., Lee, H. M., Dubois, J., Qiu, D., Hitti, J., GTC Sequencing Center Production, Finishing, and Bioinformatics Teams, Wolf, Y. I., Tatusov, R. L., Sabathe, F., Doucette-Stamm, L., Soucaille, P., Daly, M. J., Bennett, G. N., Koonin, E. V., and Smith, D. R. (2001) Genome sequence and comparative analysis of the solvent-producing bacterium *Clostridium acetobutylicum*. *J. Bacteriol. 183*, 4823−4838.
(52) Bak, D. W., and Elliott, S. J. (2014) Alternative FeS cluster ligands: tuning redox potentials and chemistry. *Curr. Opin. Chem. Biol. 19*, 50−58.
(53) Stephens, P. J., Jollie, D. R., and Warshel, A. (1996) Protein Control of Redox Potentials of Iron-Sulfur Proteins. *Chem. Rev. 96*, 2491−2514.
(54) Langen, R., Jensen, G. M., Jacob, U., Stephens, P. J., and Warshel, A. (1992) Protein control of iron-sulfur cluster redox potentials. *J. Biol. Chem. 267*, 25625−25627.
(55) Torres, R. A., Lovell, T., Noodleman, L., and Case, D. A. (2003) Density functional and reduction potential calculations of Fe4S4 clusters. *J. Am. Chem. Soc. 125*, 1923−1936.

DOI: 10.1021/acs.biochem.6b00831
Biochemistry 2016, 55, 7047−7064

(56) Battistuzzi, G., Borsari, M., Di Rocco, G., Ranieri, A., and Sola, M. (2004) Enthalpy/entropy compensation phenomena in the reduction thermodynamics of electron transport metalloproteins. *JBIC, J. Biol. Inorg. Chem. 9*, 23−26.
(57) Perrin, B. S., Miller, B. T., Schalk, V., Woodcock, H. L., Brooks, B. R., and Ichiye, T. (2014) Web-based computational chemistry education with CHARMMing III: Reduction potentials of electron transfer proteins. *PLoS Comput. Biol. 10*, e1003739.
(58) Hurley, J. K., Weber-Main, A. M., Stankovich, M. T., Benning, M. M., Thoden, J. B., Vanhooke, J. L., Holden, H. M., Chae, Y. K., Xia, B., Cheng, H., Markley, J. L., Martinez-Júlvez, M., Gomez-Moreno, C., Schmeits, J. L., and Tollin, G. (1997) Structure-function relationships in Anabaena ferredoxin: correlations between X-ray crystal structures, reduction potentials, and rate constants of electron transfer to ferredoxin:NADP+ reductase for site-specific ferredoxin mutants. *Biochemistry 36*, 11100−11117.
(59) Müller, J. J., Lapko, A., Bourenkov, G., Ruckpaul, K., and Heinemann, U. (2001) Adrenodoxin reductase-adrenodoxin complex structure suggests electron transfer path in steroid biosynthesis. *J. Biol. Chem. 276*, 2786−2789.
(60) Kurisu, G., Kusunoki, M., Katoh, E., Yamazaki, T., Teshima, K., Onda, Y., Kimata-Ariga, Y., and Hase, T. (2001) Structure of the electron transfer complex between ferredoxin and ferredoxin-NADP-(+) reductase. *Nat. Struct. Biol. 8*, 117−121.
(61) Dai, S., Friemann, R., Glauser, D. A., Bourquin, F., Manieri, W., Schürmann, P., and Eklund, H. (2007) Structural snapshots along the reaction pathway of ferredoxin-thioredoxin reductase. *Nature 448*, 92−96.
(62) Tripathi, S., Li, H., and Poulos, T. L. (2013) Structural basis for effector control and redox partner recognition in cytochrome P450. *Science 340*, 1227−1230.
(63) Hiruma, Y., Hass, M. A. S., Kikui, Y., Liu, W.-M., Ölmez, B., Skinner, S. P., Blok, A., Kloosterman, A., Koteishi, H., Löhr, F., Schwalbe, H., Nojiri, M., and Ubbink, M. (2013) The structure of the cytochrome p450cam-putidaredoxin complex determined by paramagnetic NMR spectroscopy and crystallography. *J. Mol. Biol. 425*, 4353−4365.
(64) Ashikawa, Y., Fujimoto, Z., Noguchi, H., Habe, H., Omori, T., Yamane, H., and Nojiri, H. (2006) Electron transfer complex formation between oxygenase and ferredoxin components in Rieske nonheme iron oxygenase system. *Structure 14*, 1779−1789.
(65) Acheson, J. F., Bailey, L. J., Elsen, N. L., and Fox, B. G. (2014) Structural basis for biomolecular recognition in overlapping binding sites in a diiron enzyme system. *Nat. Commun. 5*, 5009.
(66) Rumpel, S., Siebel, J. F., Diallo, M., Farès, C., Reijerse, E. J., and Lubitz, W. (2015) Structural Insight into the Complex of Ferredoxin and [FeFe] Hydrogenase from *Chlamydomonas reinhardtii*. *ChemBioChem 16*, 1663−1669.
(67) Kim, J. Y., Nakayama, M., Toyota, H., Kurisu, G., and Hase, T. (2016) Structural and mutational studies of an electron transfer complex of maize sulfite reductase and ferredoxin. *J. Biochem. 160*, 101−109.
(68) Yao, H., Wang, Y., Lovell, S., Kumar, R., Ruvinsky, A. M., Battaile, K. P., Vakser, I. A., and Rivera, M. (2012) The structure of the BfrB-Bfd complex reveals protein-protein interactions enabling iron release from bacterioferritin. *J. Am. Chem. Soc. 134*, 13470−13481.
(69) Huber, C., and Wächtershäuser, G. (1998) Peptides by activation of amino acids with CO on (Ni,Fe)S surfaces: implications for the origin of life. *Science 281*, 670−672.
(70) Imai, E., Honda, H., Hatori, K., Brack, A., and Matsuno, K. (1999) Elongation of oligopeptides in a simulated submarine hydrothermal system. *Science 283*, 831−833.
(71) Huber, C., Eisenreich, W., Hecht, S., and Wächtershäuser, G. (2003) A possible primordial peptide cycle. *Science 301*, 938−940.
(72) Davis, B. K. (2002) Molecular evolution before the origin of species. *Prog. Biophys. Mol. Biol. 79*, 77−133.
(73) Jagannathan, B., Shen, G., and Golbeck, J. H. (2012) The evolution of Type I reaction centers: the response to oxygenic photosynthesis. *Adv. Photosynth. Respir. 33*, 285−316.
(74) Hanke, G., and Mulo, P. (2013) Plant type ferredoxins and ferredoxin-dependent metabolism. *Plant, Cell Environ. 36*, 1071−1084.
(75) Green, L. S., Yee, B. C., Buchanan, B. B., Kamide, K., Sanada, Y., and Wada, K. (1991) Ferredoxin and ferredoxin-NADP reductase from photosynthetic and nonphotosynthetic tissues of tomato. *Plant Physiol. 96*, 1207−1213.
(76) Hase, T., Kimata, Y., Yonekura, K., Matsumura, T., and Sakakibara, H. (1991) Molecular cloning and differential expression of the maize ferredoxin gene family. *Plant Physiol. 96*, 77−83.
(77) Ewen, K. M., Kleser, M., and Bernhardt, R. (2011) Adrenodoxin: the archetype of vertebrate-type [2Fe-2S] cluster ferredoxins. *Biochim. Biophys. Acta, Proteins Proteomics 1814*, 111−125.
(78) Mitou, G., Higgins, C., Wittung-Stafshede, P., Conover, R. C., Smith, A. D., Johnson, M. K., Gaillard, J., Stubna, A., Münck, E., and Meyer, J. (2003) An Isc-type extremely thermostable [2Fe-2S] ferredoxin from *Aquifex aeolicus*. Biochemical, spectroscopic, and unfolding studies. *Biochemistry 42*, 1354−1364.
(79) Meyer, J., Clay, M. D., Johnson, M. K., Stubna, A., Münck, E., Higgins, C., and Wittung-Stafshede, P. (2002) A hyperthermophilic plant-type [2Fe-2S] ferredoxin from *Aquifex aeolicus* is stabilized by a disulfide bond. *Biochemistry 41*, 3096−3108.
(80) Bertini, I., Luchinat, C., Provenzani, A., Rosato, A., and Vasos, P. R. (2002) Browsing gene banks for Fe2S2 ferredoxins and structural modeling of 88 plant-type sequences: an analysis of fold and function. *Proteins: Struct., Funct., Genet. 46*, 110−127.
(81) Takubo, K., Morikawa, T., Nonaka, Y., Mizutani, M., Takenaka, S., Takabe, K., Takahashi, M.-A., and Ohta, D. (2003) Identification and molecular characterization of mitochondrial ferredoxins and ferredoxin reductase from *Arabidopsis*. *Plant Mol. Biol. 52*, 817−830.
(82) Johnson, P. J., d'Oliveira, C. E., Gorrell, T. E., and Müller, M. (1990) Molecular analysis of the hydrogenosomal ferredoxin of the anaerobic protist *Trichomonas vaginalis*. *Proc. Natl. Acad. Sci. U. S. A. 87*, 6097−6101.
(83) Moshiri, F., Crouse, B. R., Johnson, M. K., and Maier, R. J. (1995) The "nitrogenase-protective" FeSII protein of *Azotobacter vinelandii*: overexpression, characterization, and crystallization. *Biochemistry 34*, 12973−12982.
(84) Vidakovic, M. S., Fraczkiewicz, G., and Germanas, J. P. (1996) Expression and spectroscopic characterization of the hydrogenosomal [2Fe-2S] ferredoxin from the protozoan *Trichomonas vaginalis*. *J. Biol. Chem. 271*, 14734−14739.
(85) Lei, C., Rider, S. D., Wang, C., Zhang, H., Tan, X., and Zhu, G. (2010) The apicomplexan *Cryptosporidium parvum* possesses a single mitochondrial-type ferredoxin and ferredoxin:NADP+ reductase system. *Protein Sci. 19*, 2073−2084.
(86) Hoffmann, M.-C., Müller, A., Fehringer, M., Pfänder, Y., Narberhaus, F., and Masepohl, B. (2014) Coordinated expression of fdxD and molybdenum nitrogenase genes promotes nitrogen fixation by *Rhodobacter capsulatus* in the presence of oxygen. *J. Bacteriol. 196*, 633−640.
(87) Meyer, J. (2001) Ferredoxins of the third kind. *FEBS Lett. 509*, 1−5.
(88) Giastas, P., Pinotsis, N., Efthymiou, G., Wilmanns, M., Kyritsis, P., Moulis, J.-M., and Mavridis, I. M. (2006) The structure of the 2[4Fe-4S] ferredoxin from *Pseudomonas aeruginosa* at 1.32-A resolution: comparison with other high-resolution structures of ferredoxins and contributing structural features to reduction potential values. *JBIC, J. Biol. Inorg. Chem. 11*, 445−458.
(89) Emptage, M. H., Kent, T. A., Huynh, B. H., Rawlings, J., Orme-Johnson, W. H., and Münck, E. (1980) On the nature of the iron-sulfur centers in a ferredoxin from *Azotobacter vinelandii*. Mössbauer studies and cluster displacement experiments. *J. Biol. Chem. 255*, 1793−1796.
(90) Høj, P. B., Svendsen, I., Scheller, H. V., and Møller, B. L. (1987) Identification of a chloroplast-encoded 9-kDa polypeptide as a 2[4Fe-4S] protein carrying centers A and B of photosystem I. *J. Biol. Chem. 262*, 12676−12684.
(91) Schmehl, M., Jahn, A., Meyer zu Vilsendorf, A., Hennecke, S., Masepohl, B., Schuppler, M., Marxer, M., Oelze, J., and Klipp, W.

DOI: 10.1021/acs.biochem.6b00831
Biochemistry 2016, 55, 7047−7064

(1993) Identification of a new class of nitrogen fixation genes in *Rhodobacter capsulatus*: a putative membrane complex involved in electron transport to nitrogenase. *Mol. Gen. Genet. 241*, 602−615.
(92) Macedo-Ribeiro, S., Darimont, B., Sterner, R., and Huber, R. (1996) Small structural changes account for the high thermostability of 1[4Fe-4S] ferredoxin from the hyperthermophilic bacterium *Thermotoga maritima*. *Structure 4*, 1291−1301.
(93) Nielsen, M. S., Harris, P., Ooi, B. L., and Christensen, H. E. M. (2004) The 1.5 A resolution crystal structure of [Fe3S4]-ferredoxin from the hyperthermophilic archaeon *Pyrococcus furiosus*. *Biochemistry 43*, 5188−5194.
(94) Fujii, T., Hata, Y., Wakagi, T., Tanaka, N., and Oshima, T. (1996) Novel zinc-binding centre in thermoacidophilic archaeal ferredoxins. *Nat. Struct. Biol. 3*, 834−837.
(95) Atkinson, H. J., Morris, J. H., Ferrin, T. E., and Babbitt, P. C. (2009) Using sequence similarity networks for visualization of relationships across diverse protein superfamilies. *PLoS One 4*, e4345.
(96) Gerlt, J. A., Bouvier, J. T., Davidson, D. B., Imker, H. J., Sadkhin, B., Slater, D. R., and Whalen, K. L. (2015) Enzyme Function Initiative-Enzyme Similarity Tool (EFI-EST): A web tool for generating protein sequence similarity networks. *Biochim. Biophys. Acta, Proteins Proteomics 1854*, 1019−1037.
(97) Menke, M., Berger, B., and Cowen, L. (2008) Matt: local flexibility aids protein multiple structure alignment. *PLoS Comput. Biol. 4*, e10.
(98) Edgar, R. C. (2004) MUSCLE: multiple sequence alignment with high accuracy and high throughput. *Nucleic Acids Res. 32*, 1792−1797.
(99) Arabidopsis Genome Initiative (2000) Analysis of the genome sequence of the flowering plant *Arabidopsis thaliana*. *Nature 408*, 796−815.
(100) Hanke, G. T., Kimata-Ariga, Y., Taniguchi, I., and Hase, T. (2004) A post genomic characterization of *Arabidopsis* ferredoxins. *Plant Physiol. 134*, 255−264.
(101) Gou, P., Hanke, G. T., Kimata-Ariga, Y., Standley, D. M., Kubo, A., Taniguchi, I., Nakamura, H., and Hase, T. (2006) Higher order structure contributes to specific differences in redox potential and electron transfer efficiency of root and leaf ferredoxins. *Biochemistry 45*, 14389−14396.
(102) Iismaa, S. E., Vázquez, A. E., Jensen, G. M., Stephens, P. J., Butt, J. N., Armstrong, F. A., and Burgess, B. K. (1991) Site-directed mutagenesis of *Azotobacter vinelandii* ferredoxin I. Changes in [4Fe-4S] cluster reduction potential and reactivity. *J. Biol. Chem. 266*, 21563−21571.
(103) Okutani, S., Hanke, G. T., Satomi, Y., Takao, T., Kurisu, G., Suzuki, A., and Hase, T. (2005) Three maize leaf ferredoxin:NADPH oxidoreductases vary in subchloroplast location, expression, and interaction with ferredoxin. *Plant Physiol. 139*, 1451−1459.
(104) Voss, I., Goss, T., Murozuka, E., Altmann, B., McLean, K. J., Rigby, S. E. J., Munro, A. W., Scheibe, R., Hase, T., and Hanke, G. T. (2011) FdC1, a novel ferredoxin protein capable of alternative electron partitioning, increases in conditions of acceptor limitation at photosystem I. *J. Biol. Chem. 286*, 50−59.
(105) Jacquot, J. P., Suzuki, A., Peyre, J. B., Peyronnet, R., Miginiac-Maslow, M., and Gadal, P. (1988) On the specificity of pig adrenal ferredoxin (adrenodoxin) and spinach ferredoxin in electron-transfer reactions. *Eur. J. Biochem. 174*, 629−635.
(106) Tyson, C. A., Lipscomb, J. D., and Gunsalus, I. C. (1972) The role of putidaredoxin and P450 cam in methylene hydroxylation. *J. Biol. Chem. 247*, 5777−5784.
(107) Yoon, K. S., Ishii, M., Kodama, T., and Igarashi, Y. (1997) Purification and characterization of pyruvate:ferredoxin oxidoreductase from *Hydrogenobacter thermophilus* TK-6. *Arch. Microbiol. 167*, 275−279.
(108) Wan, J. T., and Jarrett, J. T. (2002) Electron acceptor specificity of ferredoxin (flavodoxin):NADP+ oxidoreductase from *Escherichia coli*. *Arch. Biochem. Biophys. 406*, 116−126.
(109) Yamamoto, M., Arai, H., Ishii, M., and Igarashi, Y. (2003) Characterization of two different 2-oxoglutarate:ferredoxin oxidoreductases from *Hydrogenobacter thermophilus* TK-6. *Biochem. Biophys. Res. Commun. 312*, 1297−1302.
(110) Guerrini, O., Burlat, B., Léger, C., Guigliarelli, B., Soucaille, P., and Girbal, L. (2008) Characterization of two 2[4Fe4S] ferredoxins from *Clostridium acetobutylicum*. *Curr. Microbiol. 56*, 261−267.
(111) Barstow, B., Agapakis, C. M., Boyle, P. M., Grandl, G., Silver, P. A., and Wintermute, E. H. (2011) A synthetic system links FeFe-hydrogenases to essential *Escherichia coli* sulfur metabolism. *J. Biol. Eng. 5*, 7.
(112) Sibbesen, O., De Voss, J. J., and Montellano, P. R. (1996) Putidaredoxin reductase-putidaredoxin-cytochrome p450cam triple fusion protein. Construction of a self-sufficient *Escherichia coli* catalytic system. *J. Biol. Chem. 271*, 22462−22469.
(113) Kumamaru, T., Suenaga, H., Mitsuoka, M., Watanabe, T., and Furukawa, K. (1998) Enhanced degradation of polychlorinated biphenyls by directed evolution of biphenyl dioxygenase. *Nat. Biotechnol. 16*, 663−666.
(114) Sakamoto, T., Joern, J. M., Arisawa, A., and Arnold, F. H. (2001) Laboratory evolution of toluene dioxygenase to accept 4-picoline as a substrate. *Appl. Environ. Microbiol. 67*, 3882−3887.
(115) Molnár, I., Jungmann, V., Stege, J., Trefzer, A., and Pachlatko, J. P. (2006) Biocatalytic conversion of avermectin into 4“-”oxo-avermectin: discovery, characterization, heterologous expression and specificity improvement of the cytochrome P450 enzyme. *Biochem. Soc. Trans. 34*, 1236−1240.
(116) Bell, S. G., Harford-Cross, C. F., and Wong, L. L. (2001) Engineering the CYP101 system for in vivo oxidation of unnatural substrates. *Protein Eng., Des. Sel. 14*, 797−802.
(117) Furukawa, K., Suenaga, H., and Goto, M. (2004) Biphenyl dioxygenases: functional versatilities and directed evolution. *J. Bacteriol. 186*, 5189−5196.
(118) Virus, C., and Bernhardt, R. (2008) Molecular evolution of a steroid hydroxylating cytochrome P450 using a versatile steroid detection system for screening. *Lipids 43*, 1133−1141.
(119) Tang, W. L., Li, Z., and Zhao, H. (2010) Inverting the enantioselectivity of P450pyr monooxygenase by directed evolution. *Chem. Commun. (Cambridge, U. K.) 46*, 5461−5463.
(120) Yonekura-Sakakibara, K., Onda, Y., Ashikari, T., Tanaka, Y., Kusumi, T., and Hase, T. (2000) Analysis of reductant supply systems for ferredoxin-dependent sulfite reductase in photosynthetic and nonphotosynthetic organs of maize. *Plant Physiol. 122*, 887−894.
(121) Navarro, F., Martín-Figueroa, E., Candau, P., and Florencio, F. J. (2000) Ferredoxin-dependent iron-sulfur flavoprotein glutamate synthase (GlsF) from the Cyanobacterium *Synechocystis sp*. PCC 6803: expression and assembly in *Escherichia coli*. *Arch. Biochem. Biophys. 379*, 267−276.
(122) Stephens, P. J., Thomson, A. J., Dunn, J. B., Keiderling, T. A., Rawlings, J., Rao, K. K., and Hall, D. O. (1978) Circular dichroism and magnetic circular dichroism of iron-sulfur proteins. *Biochemistry 17*, 4770−4778.
(123) Ta, D. T., and Vickery, L. E. (1992) Cloning, sequencing, and overexpression of a [2Fe-2S] ferredoxin gene from *Escherichia coli*. *J. Biol. Chem. 267*, 11120−11125.
(124) Petering, D. H., and Palmer, G. (1970) Properties of spinach ferredoxin in anaerobic urea solution: a comparison with the native protein. *Arch. Biochem. Biophys. 141*, 456−464.
(125) Li, B., and Elliott, S. J. (2016) The Catalytic Bias of 2-Oxoacid:ferredoxin Oxidoreductase in CO2: evolution and reduction through a ferredoxin-mediated electrocatalytic assay. *Electrochim. Acta 199*, 349−356.
(126) Ullmann, G. M., Hauswald, M., Jensen, A., and Knapp, E. W. (2000) Structural alignment of ferredoxin and flavodoxin based on electrostatic potentials: implications for their interactions with photosystem I and ferredoxin-NADP reductase. *Proteins: Struct., Funct., Genet. 38*, 301−309.
(127) Sétif, P. (2001) Ferredoxin and flavodoxin reduction by photosystem I. *Biochim. Biophys. Acta, Bioenerg. 1507*, 161−179.
(128) Hallenbeck, P. C., and Gennaro, G. (1998) Stopped-flow kinetic studies of low potential electron carriers of the photosynthetic

DOI: 10.1021/acs.biochem.6b00831
Biochemistry 2016, 55, 7047−7064

bacterium, *Rhodobacter capsulatus*: ferredoxin I and NifF. *Biochim. Biophys. Acta, Bioenerg. 1365*, 435−442.
(129) Nielsen, A. A. K., Der, B. S., Shin, J., Vaidyanathan, P., Paralanov, V., Strychalski, E. A., Ross, D., Densmore, D., and Voigt, C. A. (2016) Genetic circuit design automation. *Science 352*, aac7341.
(130) Jensen, H. M., Albers, A. E., Malley, K. R., Londer, Y. Y., Cohen, B. E., Helms, B. A., Weigele, P., Groves, J. T., and Ajo-Franklin, C. M. (2010) Engineering of a synthetic electron conduit in living cells. *Proc. Natl. Acad. Sci. U. S. A. 107*, 19213−19218.
(131) Ducat, D. C., Sachdeva, G., and Silver, P. A. (2011) Rewiring hydrogenase-dependent redox circuits in cyanobacteria. *Proc. Natl. Acad. Sci. U. S. A. 108*, 3941−3946.
(132) Agapakis, C. M., and Silver, P. A. (2010) Modular electron transfer circuits for synthetic biology: insulation of an engineered biohydrogen pathway. *Bioeng Bugs 1*, 413−418.
(133) Mellor, S. B., Nielsen, A. Z., Burow, M., Motawia, M. S., Jakubauskas, D., Møller, B. L., and Jensen, P. E. (2016) Fusion of Ferredoxin and Cytochrome P450 Enables Direct Light-Driven Biosynthesis. *ACS Chem. Biol. 11*, 1862−1869.
(134) Lassen, L. M., Nielsen, A. Z., Ziersen, B., Gnanasekaran, T., Møller, B. L., and Jensen, P. E. (2014) Redirecting photosynthetic electron flow into light-driven synthesis of alternative products including high-value bioactive natural compounds. *ACS Synth. Biol. 3*, 1−12.
(135) Nielsen, A. Z., Ziersen, B., Jensen, K., Lassen, L. M., Olsen, C. E., Møller, B. L., and Jensen, P. E. (2013) Redirecting photosynthetic reducing power toward bioactive natural product synthesis. *ACS Synth. Biol. 2*, 308−315.
(136) Zhang, J., Sonnenschein, N., Pihl, T. P. B., Pedersen, K. R., Jensen, M. K., and Keasling, J. D. (2016) Engineering an NADPH/NADP(+) Redox Biosensor in Yeast. *ACS Synth. Biol.*, DOI: 10.1021/acssynbio.6b00135.
(137) Hoff, K. G., Goodlitt, R., Li, R., Smolke, C. D., and Silberg, J. J. (2009) Fluorescence detection of a protein-bound 2Fe2S cluster. *ChemBioChem 10*, 667−670.
(138) Hoff, K. G., Culler, S. J., Nguyen, P. Q., McGuire, R. M., Silberg, J. J., and Smolke, C. D. (2009) *In vivo* fluorescent detection of Fe-S clusters coordinated by human GRX2. *Chem. Biol. 16*, 1299−1308.
(139) Vranish, J. N., Russell, W. K., Yu, L. E., Cox, R. M., Russell, D. H., and Barondeau, D. P. (2015) Fluorescent probes for tracking the transfer of iron-sulfur cluster and other metal cofactors in biosynthetic reaction pathways. *J. Am. Chem. Soc. 137*, 390−398.
(140) Pochekailov, S., Black, R. R., Chavali, V. P., Khakhar, A., and Seelig, G. (2016) A Fluorescent Readout for the Oxidation State of Electron Transporting Proteins in Cell Free Settings. *ACS Synth. Biol. 5*, 662−671.
(141) TerAvest, M. A., and Ajo-Franklin, C. M. (2016) Transforming exoelectrogens for biotechnology using synthetic biology. *Biotechnol. Bioeng. 113*, 687−697.
(142) NCBI Resource Coordinators (2016) Database resources of the National Center for Biotechnology Information. *Nucleic Acids Res. 44*, D7−D19.
(143) Pettersen, E. F., Goddard, T. D., Huang, C. C., Couch, G. S., Greenblatt, D. M., Meng, E. C., and Ferrin, T. E. (2004) UCSF Chimera–a visualization system for exploratory research and analysis. *J. Comput. Chem. 25*, 1605−1612.
(144) Quinkal, I., Davasse, V., Gaillard, J., and Moulis, J. M. (1994) On the role of conserved proline residues in the structure and function of *Clostridium pasteurianum* 2[4Fe-4S] ferredoxin. *Protein Eng., Des. Sel. 7*, 681−687.
(145) Shannon, P., Markiel, A., Ozier, O., Baliga, N. S., Wang, J. T., Ramage, D., Amin, N., Schwikowski, B., and Ideker, T. (2003) Cytoscape: a software environment for integrated models of biomolecular interaction networks. *Genome Res. 13*, 2498−2504.
(146) Caspi, R., Altman, T., Dreher, K., Fulcher, C. A., Subhraveti, P., Keseler, I. M., Kothari, A., Krummenacker, M., Latendresse, M., Mueller, L. A., Ong, Q., Paley, S., Pujar, A., Shearer, A. G., Travers, M., Weerasinghe, D., Zhang, P., and Karp, P. D. (2012) The MetaCyc database of metabolic pathways and enzymes and the BioCyc collection of pathway/genome databases. *Nucleic Acids Res. 40*, D742−53.
(147) Scherer, P. A., and Thauer, R. K. (1978) Purification and properties of reduced ferredoxin: CO2 oxidoreductase from *Clostridium pasteurianum*, a molybdenum iron-sulfur-protein. *Eur. J. Biochem. 85*, 125−135.
(148) Clark, J. E., and Ljungdahl, L. G. (1984) Purification and properties of 5,10-methylenetetrahydrofolate reductase, an iron-sulfur flavoprotein from *Clostridium formicoaceticum*. *J. Biol. Chem. 259*, 10845−10849.
(149) Bender, G., and Ragsdale, S. W. (2011) Evidence that ferredoxin interfaces with an internal redox shuttle in Acetyl-CoA synthase during reductive activation and catalysis. *Biochemistry 50*, 276−286.
(150) Gencic, S., Duin, E. C., and Grahame, D. A. (2010) Tight coupling of partial reactions in the acetyl-CoA decarbonylase/synthase (ACDS) multienzyme complex from *Methanosarcina thermophila*: acetyl C-C bond fragmentation at the a cluster promoted by protein conformational changes. *J. Biol. Chem. 285*, 15450−15463.
(151) Welte, C., Kallnik, V., Grapp, M., Bender, G., Ragsdale, S., and Deppenmeier, U. (2010) Function of Ech hydrogenase in ferredoxin-dependent, membrane-bound electron transport in *Methanosarcina mazei*. *J. Bacteriol. 192*, 674−678.
(152) Evans, M. C., Buchanan, B. B., and Arnon, D. I. (1966) A new ferredoxin-dependent carbon reduction cycle in a photosynthetic bacterium. *Proc. Natl. Acad. Sci. U. S. A. 55*, 928−934.
(153) Huber, H., Gallenberger, M., Jahn, U., Eylert, E., Berg, I. A., Kockelkorn, D., Eisenreich, W., and Fuchs, G. (2008) A dicarboxylate/4-hydroxybutyrate autotrophic carbon assimilation cycle in the hyperthermophilic Archaeum *Ignicoccus hospitalis*. *Proc. Natl. Acad. Sci. U. S. A. 105*, 7851−7856.
(154) Stadtman, T. C. (1966) Glycine reduction to acetate and ammonia: identification of ferredoxin and another low molecular weight acidic protein as components of the reductase system. *Arch. Biochem. Biophys. 113*, 9−19.
(155) Pierce, E., Becker, D. F., and Ragsdale, S. W. (2010) Identification and characterization of oxalate oxidoreductase, a novel thiamine pyrophosphate-dependent 2-oxoacid oxidoreductase that enables anaerobic growth on oxalate. *J. Biol. Chem. 285*, 40515−40524.
(156) Luque, I., Flores, E., and Herrero, A. (1993) Nitrite reductase gene from *Synechococcus sp.* PCC 7942: homology between cyanobacterial and higher-plant nitrite reductases. *Plant Mol. Biol. 21*, 1201−1205.
(157) Manzano, C., Candau, P., Gomez-Moreno, C., Relimpio, A. M., and Losada, M. (1976) Ferredoxin-dependent photosynthetic reduction of nitrate and nitrite by particles of *Anacystis nidulans*. *Mol. Cell. Biochem. 10*, 161−169.
(158) Brühl, A., Haverkamp, T., Gisselmann, G., and Schwenn, J. D. (1996) A cDNA clone from *Arabidopsis thaliana* encoding plastidic ferredoxin:sulfite reductase. *Biochim. Biophys. Acta, Protein Struct. Mol. Enzymol. 1295*, 119−124.
(159) Neumann, S., Wynen, A., Trüper, H. G., and Dahl, C. (2000) Characterization of the cys gene locus from *Allochromatium vinosum* indicates an unusual sulfate assimilation pathway. *Mol. Biol. Rep. 27*, 27−33.
(160) Sétif, P. Q., and Bottin, H. (1994) Laser flash absorption spectroscopy study of ferredoxin reduction by photosystem I in *Synechocystis sp.* PCC 6803: evidence for submicrosecond and microsecond kinetics. *Biochemistry 33*, 8495−8504.
(161) Fischer, N., Sétif, P., and Rochaix, J. D. (1997) Targeted mutations in the psaC gene of *Chlamydomonas reinhardtii*: preferential reduction of FB at low temperature is not accompanied by altered electron flow from photosystem I to ferredoxin. *Biochemistry 36*, 93−102.
(162) Jagannathan, B., and Golbeck, J. H. (2008) Unifying principles in homodimeric type I photosynthetic reaction centers: properties of PscB and the FA, FB and FX iron-sulfur clusters in green sulfur bacteria. *Biochim. Biophys. Acta, Bioenerg. 1777*, 1535−1544.

DOI: 10.1021/acs.biochem.6b00831
Biochemistry 2016, 55, 7047−7064

(163) Gutekunst, K., Chen, X., Schreiber, K., Kaspar, U., Makam, S., and Appel, J. (2014) The bidirectional NiFe-hydrogenase in *Synechocystis sp*. PCC 6803 is reduced by flavodoxin and ferredoxin and is essential under mixotrophic, nitrate-limiting conditions. *J. Biol. Chem. 289*, 1930−1937.
(164) Hedderich, R., and Forzi, L. (2006) Energy-converting [NiFe] hydrogenases: more than just H_2 activation. *J. Mol. Microbiol. Biotechnol. 10*, 92−104.
(165) Pütz, S., Dolezal, P., Gelius-Dietrich, G., Bohacova, L., Tachezy, J., and Henze, K. (2006) Fe-hydrogenase maturases in the hydrogenosomes of *Trichomonas vaginalis*. *Eukaryotic Cell 5*, 579−586.
(166) Schut, G. J., and Adams, M. W. W. (2009) The iron-hydrogenase of *Thermotoga maritima* utilizes ferredoxin and NADH synergistically: a new perspective on anaerobic hydrogen production. *J. Bacteriol. 191*, 4451−4457.
(167) Bertsch, J., Parthasarathy, A., Buckel, W., and Müller, V. (2013) An electron-bifurcating caffeyl-CoA reductase. *J. Biol. Chem. 288*, 11304−11311.
(168) Li, F., Hinderberger, J., Seedorf, H., Zhang, J., Buckel, W., and Thauer, R. K. (2008) Coupled ferredoxin and crotonyl coenzyme A (CoA) reduction with NADH catalyzed by the butyryl-CoA dehydrogenase/Etf complex from *Clostridium kluyveri*. *J. Bacteriol. 190*, 843−850.
(169) Kumagai, H., Fujiwara, T., Matsubara, H., and Saeki, K. (1997) Membrane localization, topology, and mutual stabilization of the rnfABC gene products in *Rhodobacter capsulatus* and implications for a new family of energy-coupling NADH oxidoreductases. *Biochemistry 36*, 5509−5521.
(170) Li, Q., Li, L., Rejtar, T., Lessner, D. J., Karger, B. L., and Ferry, J. G. (2006) Electron transport in the pathway of acetate conversion to methane in the marine archaeon *Methanosarcina acetivorans*. *J. Bacteriol. 188*, 702−710.
(171) Kaster, A.-K., Moll, J., Parey, K., and Thauer, R. K. (2011) Coupling of ferredoxin and heterodisulfide reduction via electron bifurcation in hydrogenotrophic methanogenic archaea. *Proc. Natl. Acad. Sci. U. S. A. 108*, 2981−2986.
(172) Wang, S., Huang, H., Moll, J., and Thauer, R. K. (2010) NADP + reduction with reduced ferredoxin and NADP+ reduction with NADH are coupled via an electron-bifurcating enzyme complex in *Clostridium kluyveri*. *J. Bacteriol. 192*, 5115−5123.
(173) Weghoff, M. C., Bertsch, J., and Müller, V. (2015) A novel mode of lactate metabolism in strictly anaerobic bacteria. *Environ. Microbiol. 17*, 670−677.
(174) Shin, M., and Arnon, D. I. (1965) Enzymic mechanisms of pyridine nucleotide reduction in chloroplasts. *J. Biol. Chem. 240*, 1405−1411.
(175) Welte, C., and Deppenmeier, U. (2011) Re-evaluation of the function of the F420 dehydrogenase in electron transport of *Methanosarcina mazei*. *FEBS J. 278*, 1277−1287.
(176) Yeremenko, N., Jeanjean, R., Prommeenate, P., Krasikov, V., Nixon, P. J., Vermaas, W. F. J., Havaux, M., and Matthijs, H. C. P. (2005) Open reading frame ssr2016 is required for antimycin A-sensitive photosystem I-driven cyclic electron flow in the cyanobacterium *Synechocystis sp*. PCC 6803. *Plant Cell Physiol. 46*, 1433−1436.
(177) Hertle, A. P., Blunder, T., Wunder, T., Pesaresi, P., Pribil, M., Armbruster, U., and Leister, D. (2013) PGRL1 is the elusive ferredoxin-plastoquinone reductase in photosynthetic cyclic electron flow. *Mol. Cell 49*, 511−523.
(178) Yamamoto, H., and Shikanai, T. (2013) In planta mutagenesis of Src homology 3 domain-like fold of NdhS, a ferredoxin-binding subunit of the chloroplast NADH dehydrogenase-like complex in *Arabidopsis*: a conserved Arg-193 plays a critical role in ferredoxin binding. *J. Biol. Chem. 288*, 36328−36337.
(179) He, Z., Zheng, F., Wu, Y., Li, Q., Lv, J., Fu, P., and Mi, H. (2015) NDH-1L interacts with ferredoxin via the subunit NdhS in Thermosynechococcus elongatus. *Photosynth. Res. 126*, 341−349.
(180) Droux, M., Jacquot, J. P., Miginac-Maslow, M., Gadal, P., Huet, J. C., Crawford, N. A., Yee, B. C., and Buchanan, B. B. (1987) Ferredoxin-thioredoxin reductase, an iron-sulfur enzyme linking light to enzyme regulation in oxygenic photosynthesis: purification and properties of the enzyme from C3, C4, and cyanobacterial species. *Arch. Biochem. Biophys. 252*, 426−439.
(181) Reher, M., Gebhard, S., and Schönheit, P. (2007) Glyceraldehyde-3-phosphate ferredoxin oxidoreductase (GAPOR) and nonphosphorylating glyceraldehyde-3-phosphate dehydrogenase (GAPN), key enzymes of the respective modified Embden-Meyerhof pathways in the hyperthermophilic crenarchaeota *Pyrobaculum aerophilum* and *Aeropyrum pernix*. *FEMS Microbiol. Lett. 273*, 196−205.
(182) van der Oost, J., Schut, G., Kengen, S. W., Hagen, W. R., Thomm, M., and de Vos, W. M. (1998) The ferredoxin-dependent conversion of glyceraldehyde-3-phosphate in the hyperthermophilic archaeon *Pyrococcus furiosus* represents a novel site of glycolytic regulation. *J. Biol. Chem. 273*, 28149−28154.
(183) Reed, G. H., Ragsdale, S. W., and Mansoorabadi, S. O. (2012) Radical reactions of thiamin pyrophosphate in 2-oxoacid oxidoreductases. *Biochim. Biophys. Acta, Proteins Proteomics 1824*, 1291−1298.
(184) Basen, M., Schut, G. J., Nguyen, D. M., Lipscomb, G. L., Benn, R. A., Prybol, C. J., Vaccaro, B. J., Poole, F. L., Kelly, R. M., and Adams, M. W. W. (2014) Single gene insertion drives bioalcohol production by a thermophilic archaeon. *Proc. Natl. Acad. Sci. U. S. A. 111*, 17618−17623.
(185) Mock, J., Zheng, Y., Mueller, A. P., Ly, S., Tran, L., Segovia, S., Nagaraju, S., Köpke, M., Dürre, P., and Thauer, R. K. (2015) Energy conservation associated with ethanol formation from H_2 and CO_2 in *Clostridium autoethanogenum* involving electron bifurcation. *J. Bacteriol. 197*, 2965−2980.
(186) Buchanan, B. B. (1969) Role of ferredoxin in the synthesis of alpha-ketobutyrate from propionyl coenzyme A and carbon dioxide by enzymes from photosynthetic and nonphotosynthetic bacteria. *J. Biol. Chem. 244*, 4218−4223.
(187) Mai, X., and Adams, M. W. (1994) Indolepyruvate ferredoxin oxidoreductase from the hyperthermophilic archaeon *Pyrococcus furiosus*. A new enzyme involved in peptide fermentation. *J. Biol. Chem. 269*, 16726−16732.
(188) Heider, J., Mai, X., and Adams, M. W. (1996) Characterization of 2-ketoisovalerate ferredoxin oxidoreductase, a new and reversible coenzyme A-dependent enzyme involved in peptide fermentation by hyperthermophilic archaea. *J. Bacteriol. 178*, 780−787.
(189) Suzuki, A., Oaks, A., Jacquot, J. P., Vidal, J., and Gadal, P. (1985) An electron transport system in maize roots for reactions of glutamate synthase and nitrite reductase: physiological and immunochemical properties of the electron carrier and pyridine nucleotide reductase. *Plant Physiol. 78*, 374−378.
(190) Kameya, M., Ikeda, T., Nakamura, M., Arai, H., Ishii, M., and Igarashi, Y. (2007) A novel ferredoxin-dependent glutamate synthase from the hydrogen-oxidizing chemoautotrophic bacterium *Hydrogenobacter thermophilus* TK-6. *J. Bacteriol. 189*, 2805−2812.
(191) Rauschenbach, R., Isernhagen, M., Noeske-Jungblut, C., Boidol, W., and Siewert, G. (1993) Cloning sequencing and expression of the gene for cytochrome P450meg, the steroid-15 beta-monooxygenase from *Bacillus megaterium* ATCC 13368. *Mol. Gen. Genet. 241*, 170−176.
(192) Wang, S., Huang, H., Kahnt, J., and Thauer, R. K. (2013) *Clostridium acidurici* electron-bifurcating formate dehydrogenase. *Appl. Environ. Microbiol. 79*, 6176−6179.
(193) Hartwich, K., Poehlein, A., and Daniel, R. (2012) The purine-utilizing bacterium *Clostridium acidurici* 9a: a genome-guided metabolic reconsideration. *PLoS One 7*, e51662.
(194) Wu, C.-H., Jiang, W., Krebs, C., and Stubbe, J. (2007) YfaE, a ferredoxin involved in diferric-tyrosyl radical maintenance in *Escherichia coli* ribonucleotide reductase. *Biochemistry 46*, 11577−11588.
(195) Anzai, Y., Saito, N., Tanaka, M., Kinoshita, K., Koyama, Y., and Kato, F. (2003) Organization of the biosynthetic gene cluster for the polyketide macrolide mycinamicin in *Micromonospora griseorubida*. *FEMS Microbiol. Lett. 218*, 135−141.

DOI: 10.1021/acs.biochem.6b00831
Biochemistry 2016, 55, 7047−7064

(196) Takamatsu, S., Xu, L.-H., Fushinobu, S., Shoun, H., Komatsu, M., Cane, D. E., and Ikeda, H. (2011) Pentalenic acid is a shunt metabolite in the biosynthesis of the pentalenolactone family of metabolites: hydroxylation of 1-deoxypentalenic acid mediated by CYP105D7 (SAV_7469) of *Streptomyces avermitilis*. *J. Antibiot. 64*, 65−71.
(197) Zhu, D., Seo, M.-J., Ikeda, H., and Cane, D. E. (2011) Genome mining in streptomyces. Discovery of an unprecedented P450-catalyzed oxidative rearrangement that is the final step in the biosynthesis of pentalenolactone. *J. Am. Chem. Soc. 133*, 2128−2131.
(198) Chang, H.-K., Mohseni, P., and Zylstra, G. J. (2003) Characterization and regulation of the genes for a novel anthranilate 1,2-dioxygenase from *Burkholderia cepacia* DBO1. *J. Bacteriol. 185*, 5871−5881.
(199) Gai, Z., Wang, X., Liu, X., Tai, C., Tang, H., He, X., Wu, G., Deng, Z., and Xu, P. (2010) The genes coding for the conversion of carbazole to catechol are flanked by IS6100 elements in *Sphingomonas sp*. strain XLDN2−5. *PLoS One 5*, e10018.
(200) Shin, K. A., and Spain, J. C. (2009) Pathway and evolutionary implications of diphenylamine biodegradation by *Burkholderia sp*. strain JS667. *Appl. Environ. Microbiol. 75*, 2694−2704.
(201) Eaton, R. W. (2001) Plasmid-encoded phthalate catabolic pathway in *Arthrobacter keyseri* 12B. *J. Bacteriol. 183*, 3689−3703.
(202) Park, D. W., Chae, J.-C., Kim, Y., Iida, T., Kudo, T., and Kim, C.-K. (2002) Chloroplast-type ferredoxin involved in reactivation of catechol 2,3-dioxygenase from *Pseudomonas sp*. S 47. *J. Biochem. Mol. Biol. 35*, 432−436.
(203) Alhapel, A., Darley, D. J., Wagener, N., Eckel, E., Elsner, N., and Pierik, A. J. (2006) Molecular and functional analysis of nicotinate catabolism in *Eubacterium barkeri*. *Proc. Natl. Acad. Sci. U. S. A. 103*, 12341−12346.
(204) Egland, P. G., Pelletier, D. A., Dispensa, M., Gibson, J., and Harwood, C. S. (1997) A cluster of bacterial genes for anaerobic benzene ring biodegradation. *Proc. Natl. Acad. Sci. U. S. A. 94*, 6484−6489.
(205) Okada, K. (2009) HO1 and PcyA proteins involved in phycobilin biosynthesis form a 1:2 complex with ferredoxin-1 required for photosynthesis. *FEBS Lett. 583*, 1251−1256.
(206) Beale, S. I., and Cornejo, J. (1991) Biosynthesis of phycobilins. 15,16-Dihydrobiliverdin IX alpha is a partially reduced intermediate in the formation of phycobilins from biliverdin IX alpha. *J. Biol. Chem. 266*, 22341−22345.
(207) Kohchi, T., Mukougawa, K., Frankenberg, N., Masuda, M., Yokota, A., and Lagarias, J. C. (2001) The *Arabidopsis* HY2 gene encodes phytochromobilin synthase, a ferredoxin-dependent biliverdin reductase. *Plant Cell 13*, 425−436.
(208) Fujita, Y. (1996) Protochlorophyllide reduction: a key step in the greening of plants. *Plant Cell Physiol. 37*, 411−421.
(209) Nagata, N., Tanaka, R., Satoh, S., and Tanaka, A. (2005) Identification of a vinyl reductase gene for chlorophyll synthesis in *Arabidopsis thaliana* and implications for the evolution of *Prochlorococcus* species. *Plant Cell 17*, 233−240.
(210) Chew, A. G. M., and Bryant, D. A. (2007) Characterization of a plant-like protochlorophyllide a divinyl reductase in green sulfur bacteria. *J. Biol. Chem. 282*, 2967−2975.
(211) Nomata, J., Mizoguchi, T., Tamiaki, H., and Fujita, Y. (2006) A second nitrogenase-like enzyme for bacteriochlorophyll biosynthesis: reconstitution of chlorophyllide a reductase with purified X-protein (BchX) and YZ-protein (BchY-BchZ) from *Rhodobacter capsulatus*. *J. Biol. Chem. 281*, 15021−15028.
(212) Scheumann, V., Schoch, S., and Rüdiger, W. (1998) Chlorophyll a formation in the chlorophyll b reductase reaction requires reduced ferredoxin. *J. Biol. Chem. 273*, 35102−35108.
(213) Wüthrich, K. L., Bovet, L., Hunziker, P. E., Donnison, I. S., and Hörtensteiner, S. (2000) Molecular cloning, functional expression and characterisation of RCC reductase involved in chlorophyll catabolism. *Plant J. 21*, 189−198.
(214) Das, D., Eser, B. E., Han, J., Sciore, A., and Marsh, E. N. G. (2011) Oxygen-independent decarbonylation of aldehydes by cyanobacterial aldehyde decarbonylase: a new reaction of diiron enzymes. *Angew. Chem., Int. Ed. 50*, 7148−7152.
(215) Johnston, J. B., Kells, P. M., Podust, L. M., and Ortiz de Montellano, P. R. (2009) Biochemical and structural characterization of CYP124: a methyl-branched lipid omega-hydroxylase from *Mycobacterium tuberculosis*. *Proc. Natl. Acad. Sci. U. S. A. 106*, 20687−20692.
(216) Cahoon, E. B., Cranmer, A. M., Shanklin, J., and Ohlrogge, J. B. (1994) delta 6 Hexadecenoic acid is synthesized by the activity of a soluble delta 6 palmitoyl-acyl carrier protein desaturase in *Thunbergia alata* endosperm. *J. Biol. Chem. 269*, 27519−27526.
(217) Cahoon, E. B., Coughlan, S. J., and Shanklin, J. (1997) Characterization of a structurally and functionally diverged acyl-acyl carrier protein desaturase from milkweed seed. *Plant Mol. Biol. 33*, 1105−1110.
(218) Li, Y., Dietrich, M., Schmid, R. D., He, B., Ouyang, P., and Urlacher, V. B. (2008) Identification and functional expression of a Delta9-fatty acid desaturase from *Psychrobacter uratívorans* in *Escherichia coli*. *Lipids 43*, 207−213.
(219) Sakamoto, T., Los, D. A., Higashi, S., Wada, H., Nishida, I., Ohmori, M., and Murata, N. (1994) Cloning of omega 3 desaturase from cyanobacteria and its use in altering the degree of membrane-lipid unsaturation. *Plant Mol. Biol. 26*, 249−263.
(220) Schmidt, H., Dresselhaus, T., Buck, F., and Heinz, E. (1994) Purification and PCR-based cDNA cloning of a plastidial n-6 desaturase. *Plant Mol. Biol. 26*, 631−642.
(221) Iba, K., Gibson, S., Nishiuchi, T., Fuse, T., Nishimura, M., Arondel, V., Hugly, S., and Somerville, C. (1993) A gene encoding a chloroplast omega-3 fatty acid desaturase complements alterations in fatty acid desaturation and chloroplast copy number of the fad7 mutant of *Arabidopsis thaliana*. *J. Biol. Chem. 268*, 24099−24105.
(222) Wada, H., Schmidt, H., Heinz, E., and Murata, N. (1993) *In vitro* ferredoxin-dependent desaturation of fatty acids in cyanobacterial thylakoid membranes. *J. Bacteriol. 175*, 544−547.
(223) Heilmann, I., Mekhedov, S., King, B., Browse, J., and Shanklin, J. (2004) Identification of the *Arabidopsis* palmitoyl-monogalactosyl-diacylglycerol delta7-desaturase gene FAD5, and effects of plastidial retargeting of *Arabidopsis* desaturases on the fad5 mutant phenotype. *Plant Physiol. 136*, 4237−4245.
(224) Kurdrid, P., Subudhi, S., Hongsthong, A., Ruengjitchatchawalya, M., and Tanticharoen, M. (2005) Functional expression of Spirulina-Delta6 desaturase gene in yeast. *Mol. Biol. Rep. 32*, 215−226.
(225) Chintalapati, S., Prakash, J. S. S., Gupta, P., Ohtani, S., Suzuki, I., Sakamoto, T., Murata, N., and Shivaji, S. (2006) A novel Delta9 acyl-lipid desaturase, DesC2, from cyanobacteria acts on fatty acids esterified to the sn-2 position of glycerolipids. *Biochem. J. 398*, 207−214.
(226) Gao, J., Ajjawi, I., Manoli, A., Sawin, A., Xu, C., Froehlich, J. E., Last, R. L., and Benning, C. (2009) FATTY ACID DESATURASE4 of *Arabidopsis* encodes a protein distinct from characterized fatty acid desaturases. *Plant J. 60*, 832−839.
(227) Zhu, X., Liu, J., and Zhang, W. (2014) *De novo* biosynthesis of terminal alkyne-labeled natural products. *Nat. Chem. Biol. 11*, 115−120.
(228) Isobe, K., Ogawa, T., Hirose, K., Yokoi, T., Yoshimura, T., and Hemmi, H. (2014) Geranylgeranyl reductase and ferredoxin from *Methanosarcina acetivorans* are required for the synthesis of fully reduced archaeal membrane lipid in *Escherichia coli* cells. *J. Bacteriol. 196*, 417−423.
(229) Seemann, M., Tse Sum Bui, B., Wolff, M., Miginiac-Maslow, M., and Rohmer, M. (2006) Isoprenoid biosynthesis in plant chloroplasts via the MEP pathway: direct thylakoid/ferredoxin-dependent photoreduction of GcpE/IspG. *FEBS Lett. 580*, 1547−1552.
(230) Okada, K., and Hase, T. (2005) Cyanobacterial non-mevalonate pathway: (E)-4-hydroxy-3-methylbut-2-enyl diphosphate synthase interacts with ferredoxin in *Thermosynechococcus elongatus* BP-1. *J. Biol. Chem. 280*, 20672−20679.

DOI: 10.1021/acs.biochem.6b00831
Biochemistry 2016, 55, 7047−7064

(231) Röhrich, R. C., Englert, N., Troschke, K., Reichenberg, A., Hintz, M., Seeber, F., Balconi, E., Aliverti, A., Zanetti, G., Köhler, U., Pfeiffer, M., Beck, E., Jomaa, H., and Wiesner, J. (2005) Reconstitution of an apicoplast-localised electron transfer pathway involved in the isoprenoid biosynthesis of *Plasmodium falciparum*. *FEBS Lett. 579*, 6433−6438.
(232) Gerjets, T., Steiger, S., and Sandmann, G. (2009) Catalytic properties of the expressed acyclic carotenoid 2-ketolases from *Rhodobacter capsulatus* and *Rubrivivax gelatinosus*. *Biochim. Biophys. Acta, Mol. Cell Biol. Lipids 1791*, 125−131.
(233) de Azevedo Wäsch, S. I., van der Ploeg, J. R., Maire, T., Lebreton, A., Kiener, A., and Leisinger, T. (2002) Transformation of isopropylamine to L-alaninol by *Pseudomonas sp*. strain KIE171 involves N-glutamylated intermediates. *Appl. Environ. Microbiol. 68*, 2368−2375.
(234) Rathinasabapathi, B., Burnet, M., Russell, B. L., Gage, D. A., Liao, P. C., Nye, G. J., Scott, P., Golbeck, J. H., and Hanson, A. D. (1997) Choline monooxygenase, an unusual iron-sulfur enzyme catalyzing the first step of glycine betaine synthesis in plants: prosthetic group characterization and cDNA cloning. *Proc. Natl. Acad. Sci. U. S. A. 94*, 3454−3458.
(235) Cryle, M. J., Bell, S. G., and Schlichting, I. (2010) Structural and biochemical characterization of the cytochrome P450 CypX (CYP134A1) from *Bacillus subtilis*: a cyclo-L-leucyl-L-leucyl dipeptide oxidase. *Biochemistry 49*, 7282−7296.
(236) Weeratunga, S. K., Gee, C. E., Lovell, S., Zeng, Y., Woodin, C. L., and Rivera, M. (2009) Binding of *Pseudomonas aeruginosa* apobacterioferritin-associated ferredoxin to bacterioferritin B promotes heme mediation of electron delivery and mobilization of core mineral iron. *Biochemistry 48*, 7420−7431.
(237) Kim, J. H., Frederick, R. O., Reinen, N. M., Troupis, A. T., and Markley, J. L. (2013) [2Fe-2S]-ferredoxin binds directly to cysteine desulfurase and supplies an electron for iron-sulfur cluster assembly but is displaced by the scaffold protein or bacterial frataxin. *J. Am. Chem. Soc. 135*, 8117−8120.
(238) Webert, H., Freibert, S.-A., Gallo, A., Heidenreich, T., Linne, U., Amlacher, S., Hurt, E., Mühlenhoff, U., Banci, L., and Lill, R. (2014) Functional reconstitution of mitochondrial Fe/S cluster synthesis on Isu1 reveals the involvement of ferredoxin. *Nat. Commun. 5*, 5013.
(239) Crossnoe, C. R., Germanas, J. P., LeMagueres, P., Mustata, G., and Krause, K. L. (2002) The crystal structure of *Trichomonas vaginalis* ferredoxin provides insight into metronidazole activation. *J. Mol. Biol. 318*, 503−518.
(240) Hannemann, F., Bera, A. K., Fischer, B., Lisurek, M., Teuchner, K., and Bernhardt, R. (2002) Unfolding and conformational studies on bovine adrenodoxin probed by engineered intrinsic tryptophan fluorescence. *Biochemistry 41*, 11008−11016.
(241) Sheftel, A. D., Stehling, O., Pierik, A. J., Elsässer, H.-P., Mühlenhoff, U., Webert, H., Hobler, A., Hannemann, F., Bernhardt, R., and Lill, R. (2010) Humans possess two mitochondrial ferredoxins, Fdx1 and Fdx2, with distinct roles in steroidogenesis, heme, and Fe/S cluster biosynthesis. *Proc. Natl. Acad. Sci. U. S. A. 107*, 11775−11780.
(242) Schiffler, B., Bureik, M., Reinle, W., Müller, E.-C., Hannemann, F., and Bernhardt, R. (2004) The adrenodoxin-like ferredoxin of *Schizosaccharomyces pombe* mitochondria. *J. Inorg. Biochem. 98*, 1229−1237.
(243) Sainz, G., Jakoncic, J., Sieker, L. C., Stojanoff, V., Sanishvili, N., Asso, M., Bertrand, P., Armengaud, J., and Jouanneau, Y. (2006) Structure of a [2Fe-2S] ferredoxin from *Rhodobacter capsulatus* likely involved in Fe-S cluster biogenesis and conformational changes observed upon reduction. *JBIC, J. Biol. Inorg. Chem. 11*, 235−246.
(244) Reipa, V., Holden, M. J., Mayhew, M. P., and Vilker, V. L. (2000) Temperature dependence of the formal reduction potential of putidaredoxin. *Biochim. Biophys. Acta, Bioenerg. 1459*, 1−9.
(245) Jung, Y. S., Gao-Sheridan, H. S., Christiansen, J., Dean, D. R., and Burgess, B. K. (1999) Purification and biophysical characterization of a new [2Fe-2S] ferredoxin from *Azotobacter vinelandii*, a putative [Fe-S] cluster assembly/repair protein. *J. Biol. Chem. 274*, 32402−32410.
(246) Armengaud, J., Meyer, C., and Jouanneau, Y. (1994) Recombinant expression of the fdxD gene of *Rhodobacter capsulatus* and characterization of its product, a [2Fe-2S] ferredoxin. *Biochem. J. 300* (Part 2), 413−418.
(247) Cammack, R., Rao, K. K., Bargeron, C. P., Hutson, K. G., Andrew, P. W., and Rogers, L. J. (1977) Midpoint redox potentials of plant and algal ferredoxins. *Biochem. J. 168*, 205−209.
(248) Matsumura, T., Kimata-Ariga, Y., Sakakibara, H., Sugiyama, T., Murata, H., Takao, T., Shimonishi, Y., and Hase, T. (1999) Complementary DNA cloning and characterization of ferredoxin localized in bundle-sheath cells of maize leaves. *Plant Physiol. 119*, 481−488.
(249) Tagawa, K., and Arnon, D. I. (1968) Oxidation-reduction potentials and stoichiometry of electron transfer in ferredoxins. *Biochim. Biophys. Acta, Bioenerg. 153*, 602−613.
(250) Kyritsis, P., Hatzfeld, O. M., Link, T. A., and Moulis, J. M. (1998) The two [4Fe-4S] clusters in *Chromatium vinosum* ferredoxin have largely different reduction potentials. Structural origin and functional consequences. *J. Biol. Chem. 273*, 15404−15411.
(251) Unciuleac, M., Boll, M., Warkentin, E., and Ermler, U. (2004) Crystallization of 4-hydroxybenzoyl-CoA reductase and the structure of its electron donor ferredoxin. *Acta Crystallogr., Sect. D: Biol. Crystallogr. 60*, 388−391.
(252) Yu, L., Vassiliev, I. R., Jung, Y. S., Bryant, D. A., and Golbeck, J. H. (1995) Modified ligands to FA and FB in photosystem I. II. Characterization of a mixed ligand [4Fe-4S] cluster in the C51D mutant of PsaC upon rebinding to P700-Fx cores. *J. Biol. Chem. 270*, 28118−28125.
(253) Mullinger, R. N., Cammack, R., Rao, K. K., Hall, D. O., Dickson, D. P., Johnson, C. E., Rush, J. D., and Simopoulos, A. (1975) Physicochemical characterization of the four-iron-four-sulphide ferredoxin from *Bacillus stearothermophilus*. *Biochem. J. 151*, 75−83.
(254) Iwasaki, T., Wakagi, T., Isogai, Y., Tanaka, K., Iizuka, T., and Oshima, T. (1994) Functional and evolutionary implications of a [3Fe-4S] cluster of the dicluster-type ferredoxin from the thermoacidophilic archaeon, *Sulfolobus sp*. strain 7. *J. Biol. Chem. 269*, 29444−29450.

DOI: 10.1021/acs.biochem.6b00831
Biochemistry 2016, 55, 7047−7064